AD-A129 693 SCATTERING OF RADAR WAVES BY MINE FIELDS(U) GEO ELECTROMAGNETICS INC BERKELEY CA M A MORGAN 1980 DAAK70-80-C-0039 1/1

UNCLASSIFIED F/G 17/9 NL

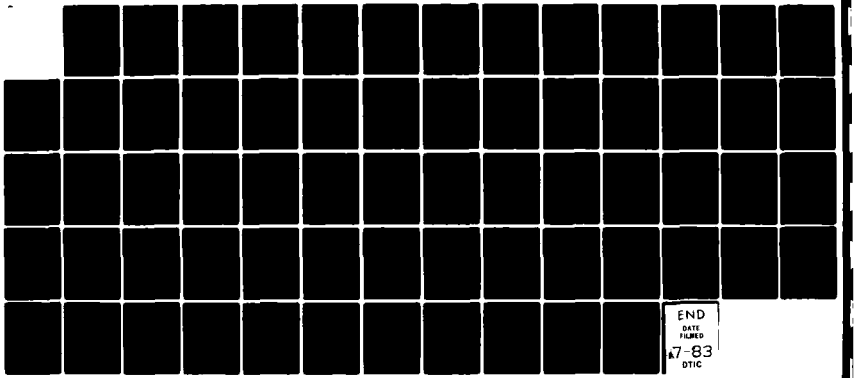

END
DATE FILMED
7-83
DTIC

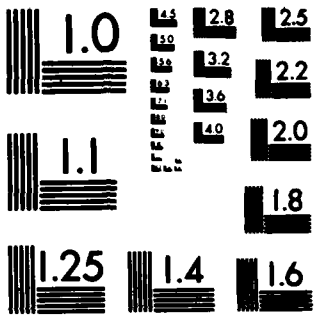

(12)

SCATTERING OF RADAR WAVES BY MINE FIELDS

A Final Report Submitted to

U.S. Army Mobility Equipment Research
and Development Command
Contract No. DAAK70-80-C-0039

by

M.A. Morgan, Ph.D.

Geo Electromagnetics, Inc.
P.O. Box 679
Berkeley, CA 94701

SCATTERING OF RADAR WAVES BY MINE FIELDS

A Final Report Submitted to

U.S. Army Mobility Equipment Research
and Development Command
Contract No. DAAK70-80-C-0039

1980

by

M.A. Morgan, Ph.D.

Geo Electromagnetics, Inc.
P.O. Box 679
Berkeley, CA 94701

The views, opinions, and/or findings contained in the report are those of the authors and should not be construed as an official Department of the Army position, policy, or decision, unless so designated by other documentation.

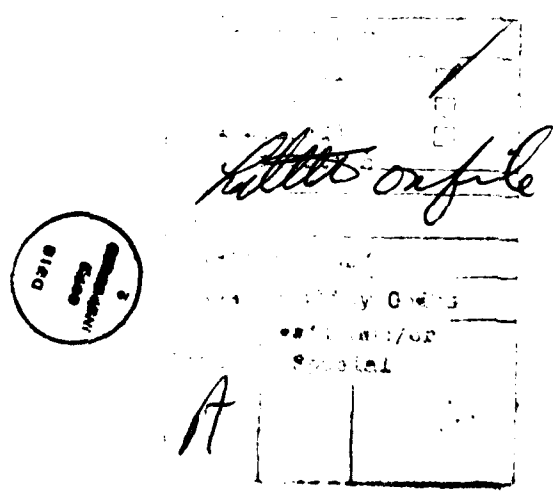

Abstract

Radar scattering by an array of surface land mines is studied. The array is considered to be a random perturbation of a uniform array. The analytical evaluation of the expectation is performed for this problem under specified, but realistic, assumptions. The analytic expression for the expectation contains coherent and incoherent array factors, each of which are summations of terms that are weighted by the effect of the antenna pattern. By curve fitting the antenna gain pattern with exponential functions in elevation and azimuth the resultant series are summable. The resultant expression for normalized signal to clutter ratio displays the coherent contributions from the radar system parameters (such as, beamwidths, frequencies, depression angle and pulse width) in conjunction with the randomness of mine placement and the clutter distribution.

TABLE OF CONTENTS

I. INTRODUCTION

Our goal in this work is to investigate the process of detection of randomly spaced mines as a function of the deterministic and statistical parameters of the radar, mine distribution and ground clutter. The main reason for such an undertaking is to provide information for optimal design of radar systems and their implementation in the mine field mapping process.

As is common for surface mapping radars the clutter echoes are dominant over system generated noise and a key parameter in defining the radar system performance is the echo signal power to clutter ration S/C [1; Chap. 13] To evaluate this ratio, as indicated in the proposal, requires the computation of the time-average radar echo power as contributed by the randomly placed scatterers in the range-azimuth cell of the radar as the antenna beam and platform both slowly change their positions. Since the statistical system being considered may be assumed to be ergodic this time-average calculation can be replaced with a statistical evaluation of expectation over the ensemble of all possible random mine placements.

There are two common methods of computing the ensemble expectations: direct analytic evaluation and Monte-Carlo simulation. The direct analytic technique requires a probability density description of all the random variables of the system and becomes easily intractable for complicated systems having mutual dependencies between the variables. The Monte-Carlo method requires a model of how the various possible system configurations evolve in nature as outcomes of the random process. The model is simulated repeatedly using appropriately distributed random number generators for the variables and expectations are obtained by averaging the outcomes.

As originally envisioned, the expectation evaluation was to be attempted by analytic means with the Monte-Carlo method as a backup in case of failure in the analytic technique. As will be shown, the analytical evaluation of the expectation can be performed for this problem using certain specified, but realistic, assumptions. The analytic expression for the expectation contains coherent and incoherent array factors which are each summations of weighted (by the antenna pattern) coherent and incoherent terms due to scattering from the centroid positions of each scatterer in the mine array. By curve fitting the gain pattern with a decaying exponential in elevation and azimuth it is possible to transform these two summations into geometric series which are then summed in closed form. The resultant expression for normalized S/C displays the inherent contributions from radar system parameters (such as beamwidths, frequency, depression angle, and pulse width) in conjunction with the randomness of mine placement and the clutter distribution.

The presentation that follows has been organized for optimum useful information conveyance with the results of this work being displayed in the next section along with a discussion of trends and observations. A more detailed set of conclusions as well as details of the analysis that was performed is left to the final section wherein a tutorial format is utilized to accommodate a wider readership. Some mathematical details, a special case, computer programs and description of notation are relegated to appendices. Finally, several references covering electromagnetics, radar systems, radar cross-section and clutter properties, probability theory and scattering by random media are included for use by readers and are cited where appropriate in the text.

II. RESULTS AND OBSERVATIONS

In order for the results to be meaningful we must first consider the pertinent assumptions and definitions involved in their derivation. The actual derivation, however, will be left until Section IV.

In Figure 1 the geometry of the assumed model is depicted. The radar system antenna illuminates a patch of the mine field with the centroid of the main beam (antenna boresight) pointing towards the origin of the cartesian coordinate system. The mine field is assumed to extend over some irregular shaped region of the x-y plane, Ω, covering many range-azimuth cells of the projected radar beam on the surface. A range-azimuth cell is depicted in part (b) of Figure 1. Assuming that the depression angle to the main beam look direction is θ_0 and that the range to the surface centroid point is R_0, as shown, then the surface projection of the half-power contour of the main beam will appear as in Figure 1(b), where θ_B is the vertical elevation (EL) half-power (3 dB) beamwidth and ϕ_B is the horizontal azimuth (AZ) 3 dB beamwidth, both expressed in radians. The range-azimuth cell is limited in range by the effective temporal pulse-width of the radar, τ. The time gating of the radar receiver allows range resolution of two point targets by as little as $c\tau/2$, where $c = 3 \times 10^8$ m/sec. On the surface, which is slanted with respect to the look direction to the radar, this resolution translates to $(c\tau \sec \theta_0)/2$ in surface range. The echo returns from both the mines and clutter will be produced from an illuminated surface patch with width of several azimuth beamwidths but time-windowed at one projected range cell. For large depression angles (looking almost straight down) the patch range will be limited by several elevation beamwidths of the antenna, since $(c\tau \sec \theta_0)/2$ becomes infinite.

Figure 1. The Model Geometry

(a) Radar and Mine Field

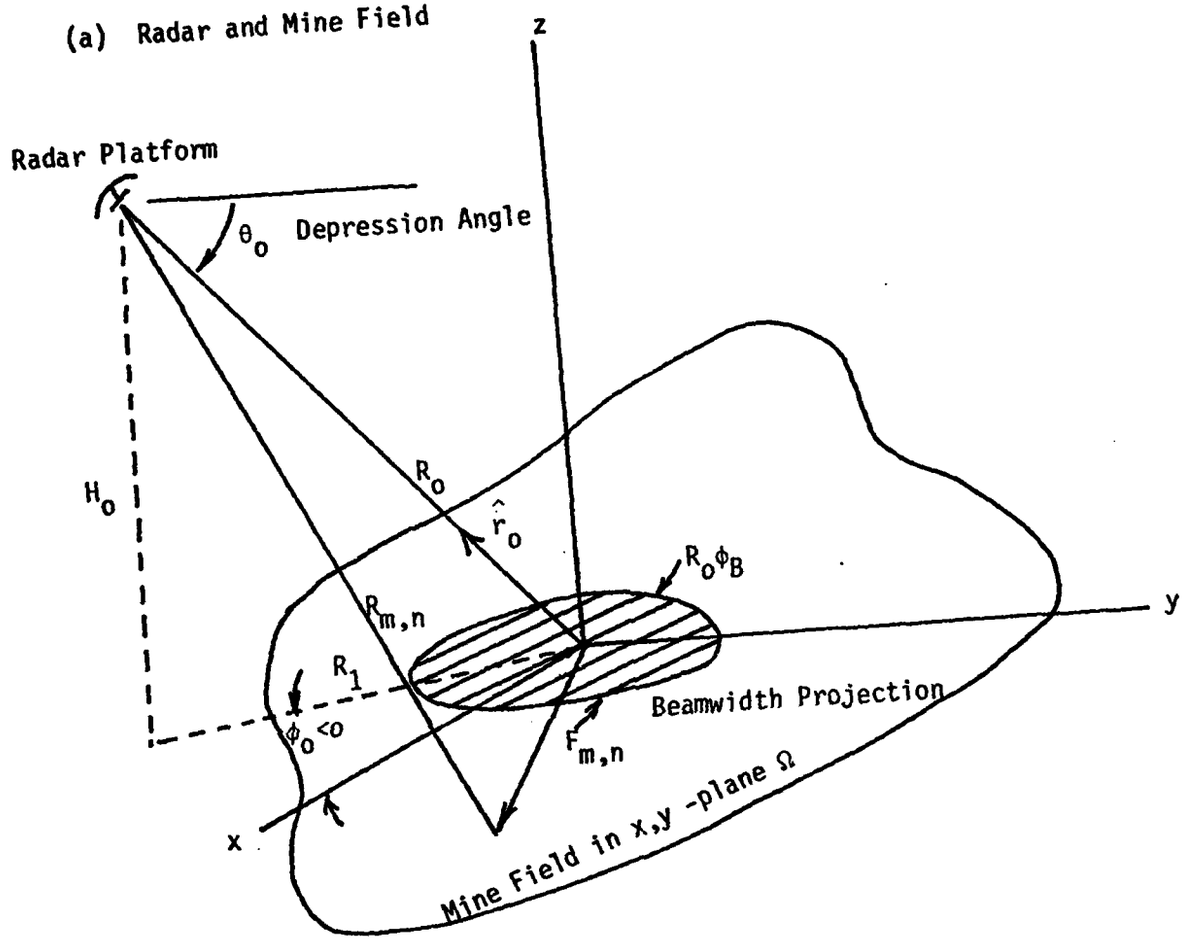

(b) Beam Projection

Beamwidth Elevation Projection

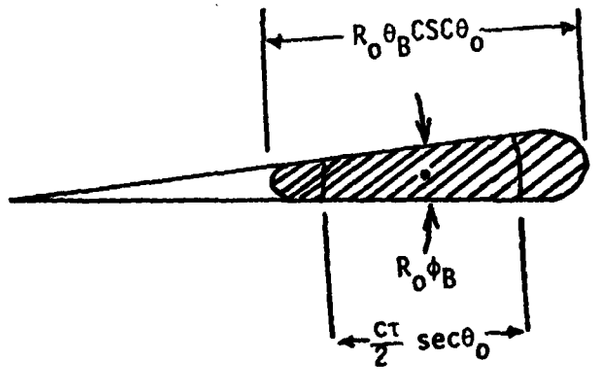

Range-Cell Projection

ϕ_B = AZ 3dB Beamwidth

θ_B = EL 3dB Beamwidth

τ = Pulse width

$c = 3 \times 10^8$ m/sec

Note: The range-cell projection can be larger or smaller than the beam width elevation projection depending on θ_o.

The mine placement is statistical. To model this situation on a usable basis we assume that the mine positions are randomly perturbed from some specific position grid, as would be the case when mines are laid on a systematic basis by moving from one position to another. The centroid grid will be assumed to be rectangular with spacing of dx and dy. From each of these centroid positions a mine is "thrown" randomly with its relative x and y coordinates having a zero-mean gaussian probability density with respective standard deviations of σ_x and σ_y.

The electromagnetic echo from the mine field is simply a linear sum of terms from each of the random mines. This sum, if containing a large enough number of mines, can be replaced for computational purposes with statistical expectation over the joint probability density function of the mine-field ensemble. This expectation is considered in general and evaluated in closed form in Section IV for a special case of practical significance where the antenna gain pattern can be approximated in vertical and horizontal off-boresight angles by an exponentially tapered function. A key result from Section IV is that the radar cross section (RCS) of a mine field composed of identical mines, each having the same independent RCS_o is of the form

$$RCS_M = RCS_o \cdot F \qquad (1)$$

where F is an array factor which is a function of the statistics of the mine field (standard deviation of mine placements vs. wavelength of the incident field) but is independent of the individual mine structure and RCSM is the radar cross section of the mine field. A common assumption in taking expectations of random scatterers is that the total scattered power is simply the sum of the individual powers returned from each of the scatterers, [2; pp. 77-80]. This is termed the "incoherent" scattering assumption and is valid when the standard deviations are much

larger than the wavelength of the illuminating field. On the other extreme, when the standard deviations are much smaller than the wavelength, the random displacements of the mines from their centroids do not appreciably perturb the phases of the individual fields from each of the scatterers. A good approximation is then to simple add the fields from each of the mines placed at its respective centroid. This is termed the "coherent" approximation since the individual fields add coherently with specific and known relative phases. As is shown in Section IV the array factor, F, in equation (1) can be expressed as a weighted sum of incoherent and coherent case array factors with the relative proportions (weights) depending upon the "randomness" of the distribution of mines

$$F = e^{-\gamma^2} F_c + (1 - e^{-\gamma^2}) F_I \tag{2a}$$

where

$$\gamma = 4\pi \frac{\sigma_o}{\lambda_o} \cos \theta_o \tag{2b}$$

for the case of equal standard deviations $\sigma_x = \sigma_y = \sigma_o$ with λ_o the wavelength of the incident field and θ_o the depression angle. Note that as σ_o/λ_o grows (increase randomness) the contribution of the incoherent term F_I increases relative to that of the coherent term F_c. Note also that as θ_o approaches 90° (look-down incidence) γ goes to zero and $F \rightarrow F_c$. This is true because at straight-down incidence random perturbations of mine positions at right angles to the platform direction do not, under the far-field assumption, change the path lengths or phases of the echo returns from those of their values for centroid located mines.

Coincident with the echo signal from the mines will be reflected power from the earth and other objects colocated with the mine field such as trees, vegetation and perhaps man-made structures. This unwanted echo tends to mask that of the mines and

is thus termed "clutter" due to its cluttering effect on radar observation screens. The ratio of signal power to clutter power S/C is thus an important quantity for radar performance. As is shown in Section IV this power ratio depends upon the ratio of mine field cross section to that of the clutter returns

$$\frac{S}{C} = \frac{RCS_M}{RCS_C} \tag{3}$$

The effects of distance and antenna gain are not explicit in this ratio since these terms are common to both the mines and the colocated clutter scatterers, and thus cancel.

It is common to express clutter cross section as a ratio of cross section per physical surface area, RCS'_C, [3]. Using this concept it is shown in Section IV that the signal to clutter power ratio is given by

$$\frac{S}{C} = \frac{RCS_o}{RCS'_C \, dx \, dy} \left\{ 1 + e^{-\gamma^2 \left(\frac{F_c}{F_I} - 1 \right)} \right\} \tag{4}$$

Note that in the limit of increasing randomness of mine placements (γ large) the S/C becomes simply the ratio of the individual mine RCS per unit area (there is one mine having RCS_o per grid square of area dx dy) to the clutter RCS per unit area. This is the incoherent limit. For $\gamma \to 0$ (little randomness) we have

$$\lim_{\gamma \to 0} \frac{S}{C} = \frac{RCS_o \cdot F_c}{dx \, dy \cdot RCS'_C \cdot F_I} \tag{5}$$

This is true because the mines have coherent array factors F_c while the clutter per unit square has the same incoherent array factor F_I as the mines had under highly random conditions. Under the condition of γ large the F_I's in the numerator and denominator cancelled leaving only the ratios of cross sections per unit area. These facts will be shown explicitly in Section IV.

The term in curly brackets in (4), given by

$$I = \left\{ 1 + e^{-\gamma^2} \left(\frac{F_c}{F_I} - 1 \right) \right\} \tag{6}$$

will be termed the signal to clutter "improvement factor" since it is unity under the incoherent assumption. Because of partially coherent addition of random fields at specific frequencies for a given depression angle this improvement factor can become very large--it can also become less than unity at certain frequencies, as will be seen. As frequency is increased it ultimately approaches unity in all cases except when the mine placement is "deterministic" ($\sigma_o = 0$).

The advantage of writing the S/C in terms of an improvement factor is that all characteristics of the individual mines and particular mine field clutter conditions are contained in the cross section ratio while the improvement factor, I, is independent of the types of mines and local clutter conditions but does depend upon the array size, randomness, frequency and gain pattern of the radar antenna over the illuminated area. The S/C is simply its value under "incoherent conditions" times I.

In addition to the periodic frequencies for resonances and antiresonances of the improvement factor, to be displayed shortly, the individual mines will have resonant behavior in RCS_o over a band of frequencies. This band of frequencies for mine resonances will in almost all foreseeable cases be observed at much higher frequencies than that of the resonant band for the grid improvement factor, I. At these higher mine resonant frequencies the improvement factor will be close to unity. This topic is discussed more extensively in the final section (IV.E) of this report and is also considered in detail in a separate contract with Geo Electromagnetics.

To produce quantitative results several cases of computation were performed for the mine field signal to clutter improvement

factor given by equation (6). Two special classes of geometry are considered. Class I considers cases where the mine field extent is large compared to the range-azimuth cell size on the surface while Class II considers the opposite case of mine field size much smaller than the range-azimuth cell size. In all cases under both classes the geometry was specialized to that of Figure 2 with the radar platform located a surface distance of R_1 from the beam center ground point while at altitude H_o. A locally flat surface is assumed.

Some representative computations of improvement factor for the mine field array factor are shown in Figures 3 through 13. This set of results, although not exhaustive by any means, does indicate the general relationships between improvement factor as a function of frequency and certain key parameters.

The fixed parameters in all cases are:

R_1 = 1000 meters (ground distance from platform to centroid of main beam on the ground)

dx = dy = 1.51 meters (rectangular grid spacing for centroid of random mine positions)

FREQ. RANGE = 10 MHz to 510 MHz plotted in 1 MHz increments (501 points total)

In Figures 3 through 8 Class I (mine field much larger in extent than the range-azimuthal cell size of the radar) is considered and in Figures 9 through 13 Class II (mine field much smaller than the range-azimuthal cell size of the radar) is considered. The signal to clutter improvement factor (equation (6)) is plotted versus frequency in Figures 1 through 8 and the array factor F (equation (2a)) is plotted in Figures 9 through 13.

Figure 2. Specialized Geometry

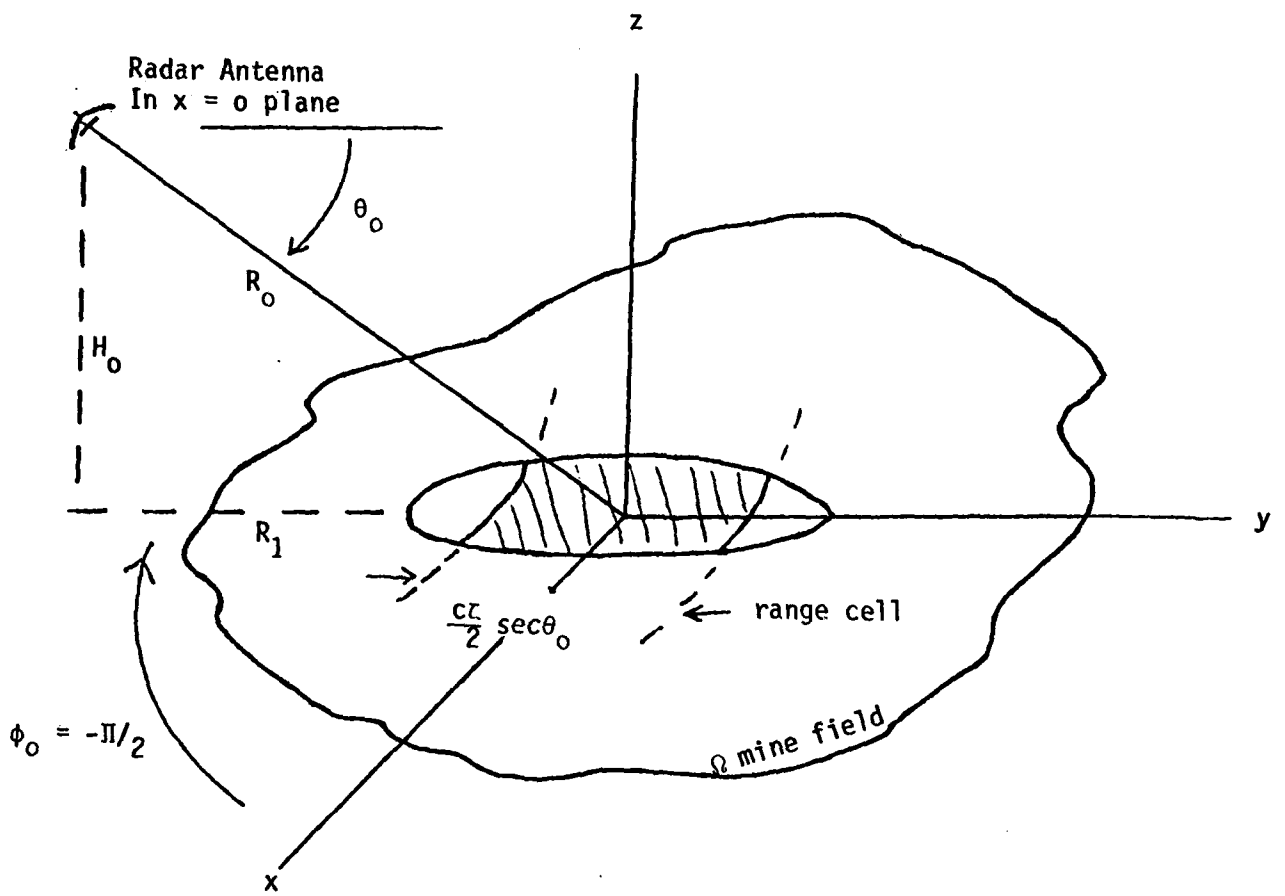

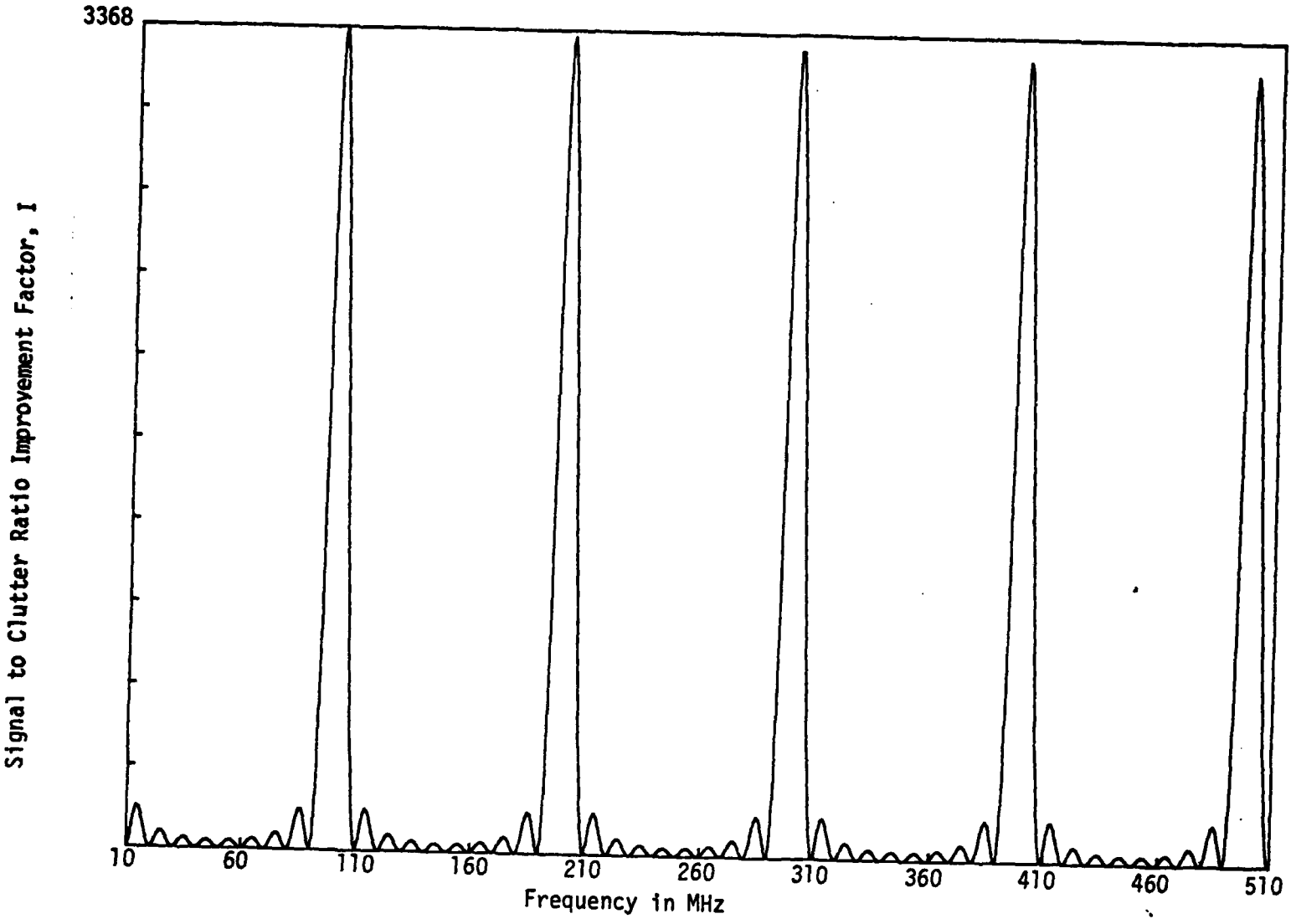

Figure 3. Plot of I vs. Frequency at H_o = 100 m, R_1 = 1000 m, ϕ_B = 5° θ_B = 5°, dx = 1.51 m, dy = 1.51m, σ_o = .01 m, τ = 0.1 μsec

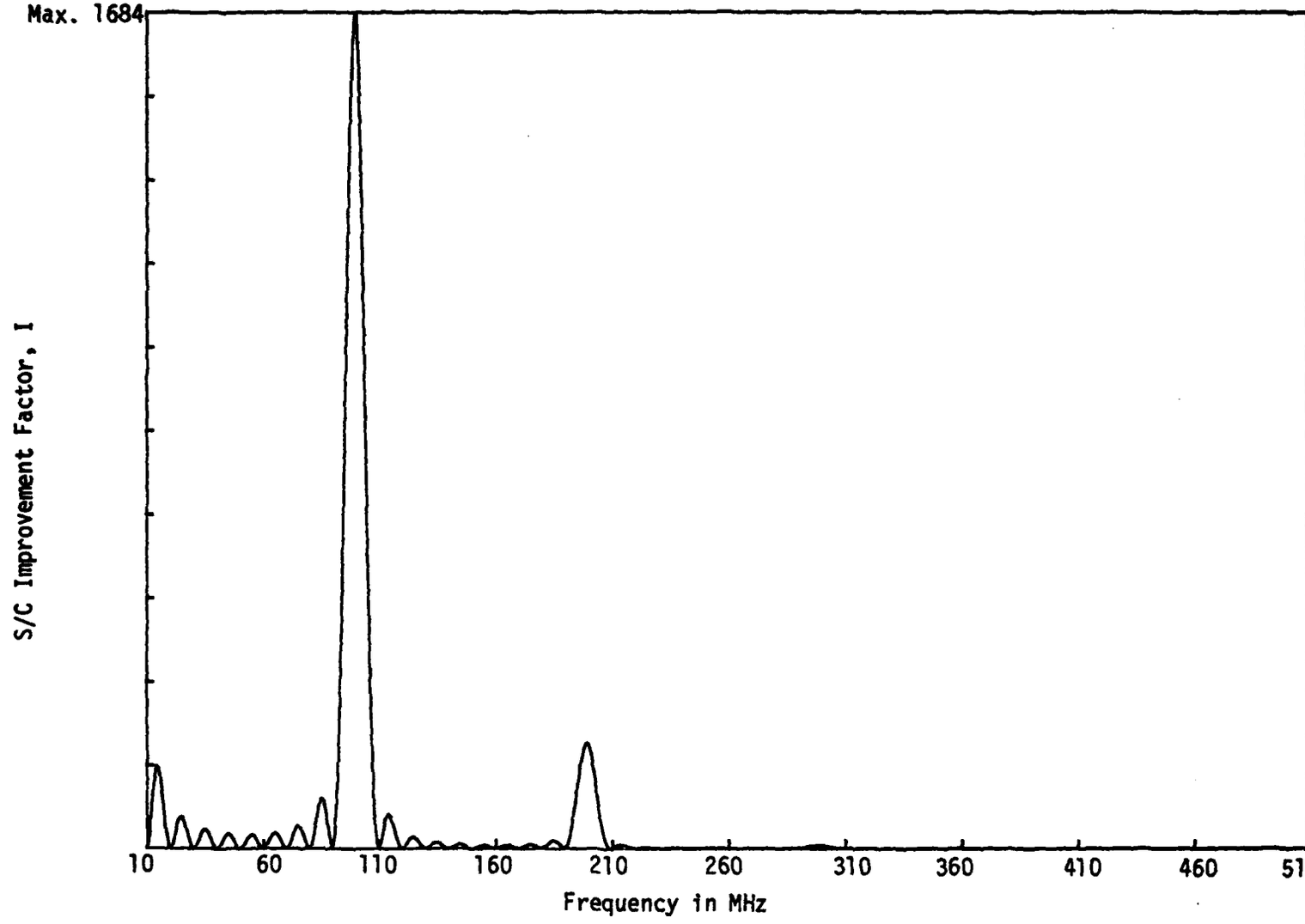

Figure 4. Plot of I vs Frequency using same parameters as in Figure 3, except σ_o = .2 m, i.e., H_o = 100 m, R_1 = 1000 m, ϕ_B = 5°, θ_B = 5°, dx = dy = 1.51m, $\sigma_x = \sigma_y = \sigma_o$ = 0.2 m τ = .1 μsec.

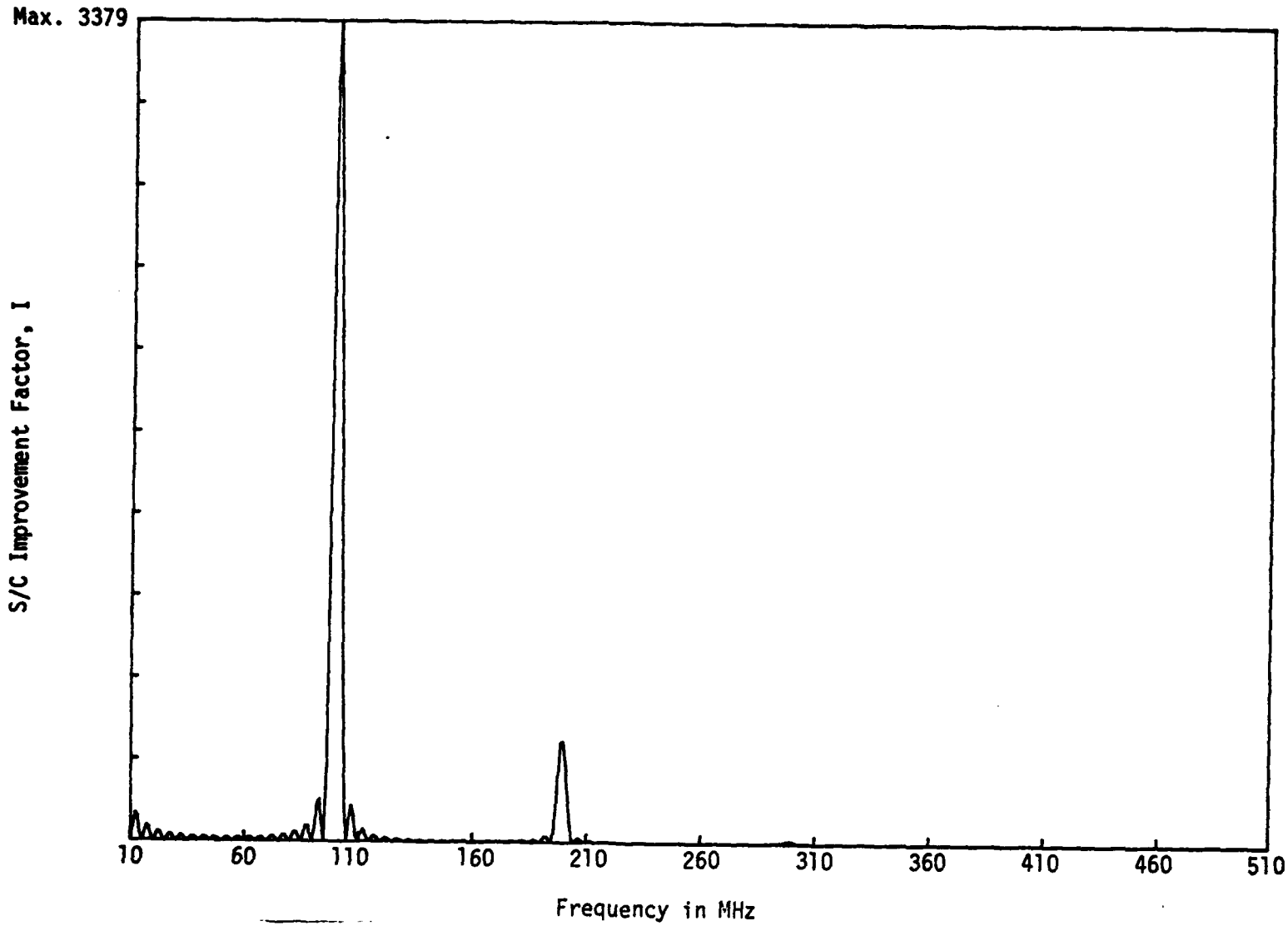

Figure 5. Plot of I vs. Frequency using same parameters as in Figure 4, except τ = .2 μsec

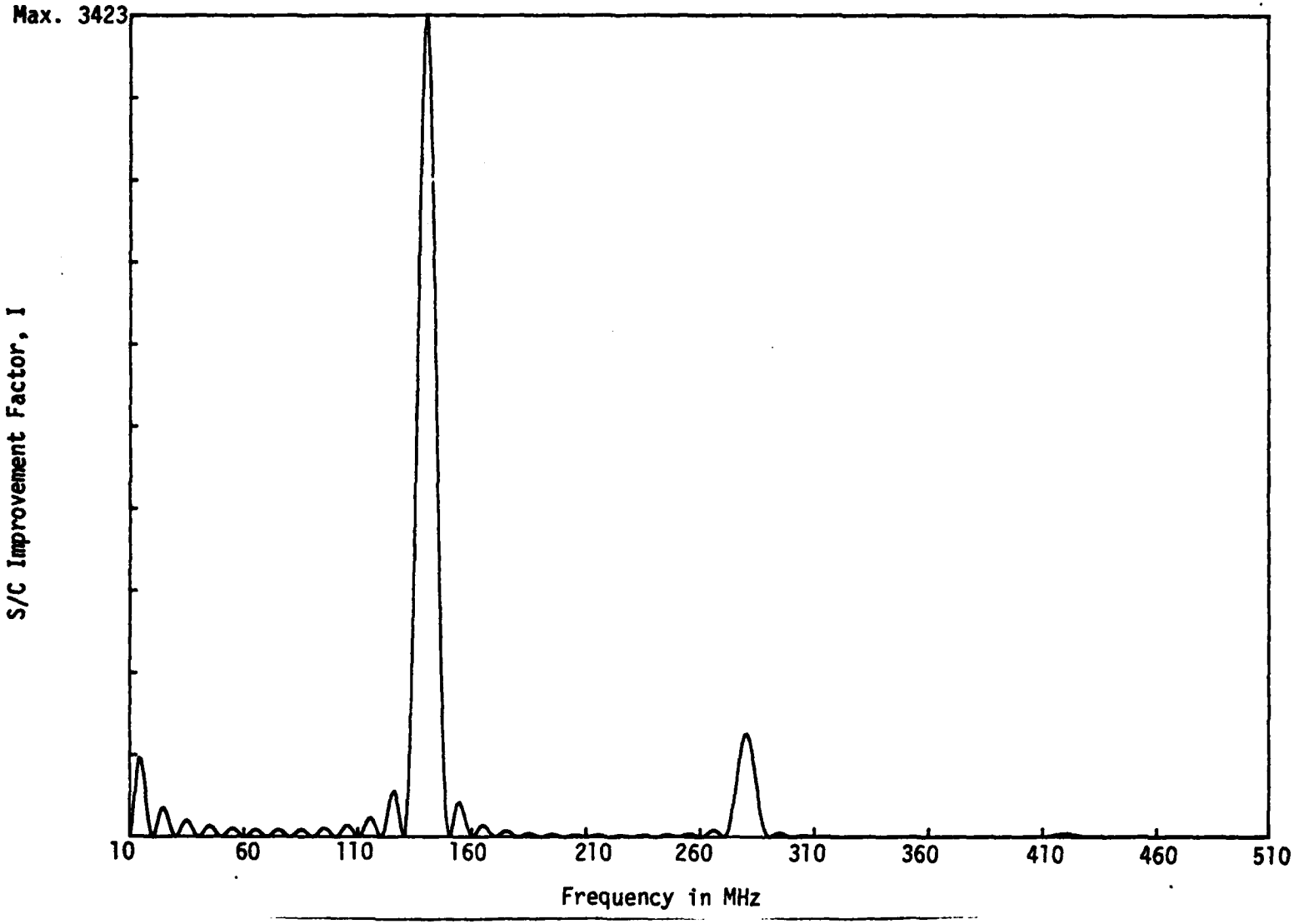

Figure 6. Plot of I vs. Frequency using same parameters as Figure 4, except H_o = 1000 m

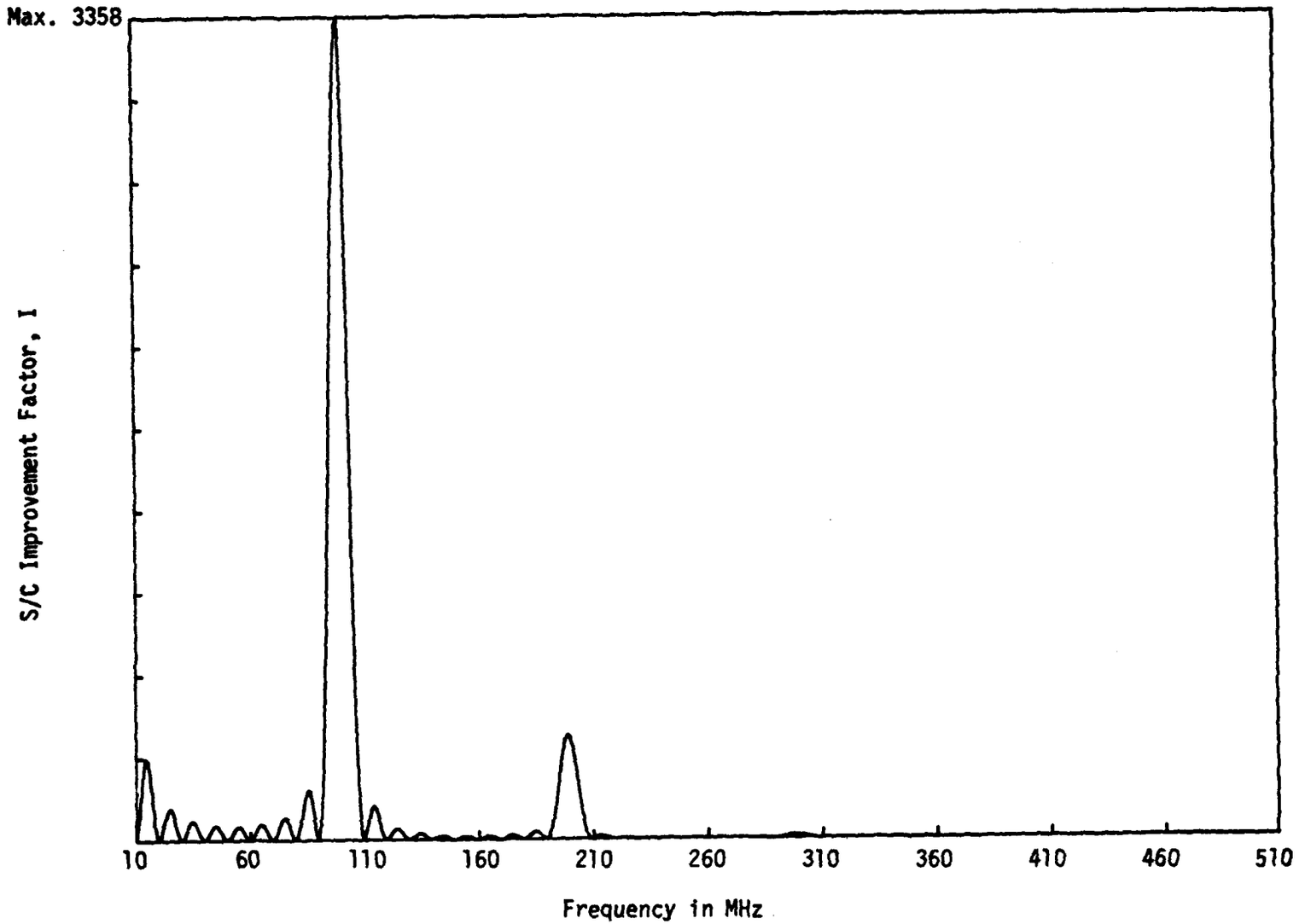

Figure 7. Plot of I vs. Frequency using same parameters as in Figure 4, except $\theta_B = 10°$ and $\phi_B = 10°$

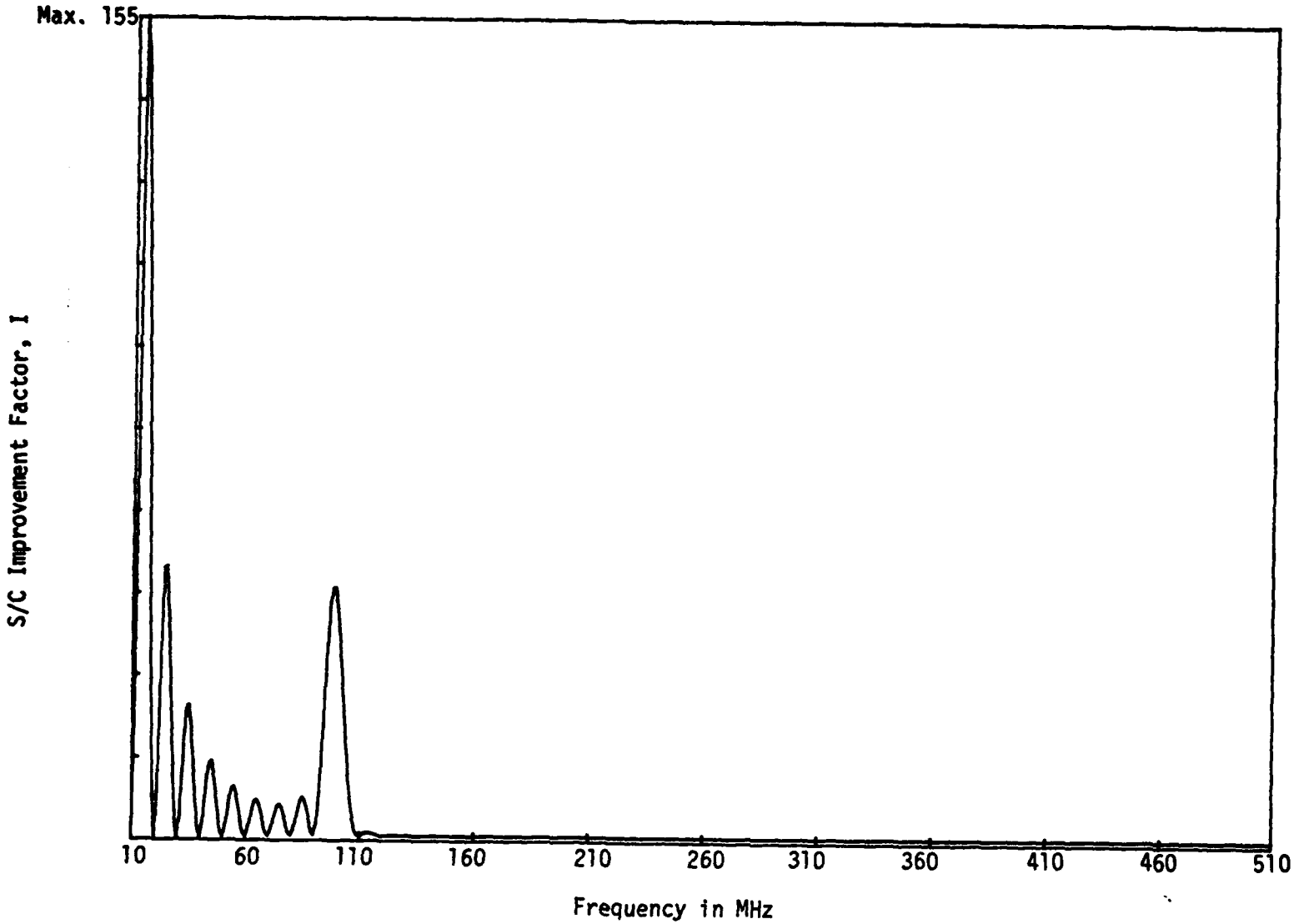

Figure 8. Plot of I vs. Frequency using same parameters as in Figure 3, except σ_o = .5 m

The parameters being varied, one at a time, are platform height H_o, antenna azimuth beamwidth ϕ_B, and mine placement standard deviation, σ_o, as well as radar pulse width, τ. The standard canonical or baseline whose spectra is displayed in Figure 4 has parameters

H_o = 100 meters (near grazing incidence)

ϕ_B = 5 degrees (narrow at the HF and VHF frequencies being considered)

σ_o = 0.2 meters

τ = 0.1 μsec

Table I summarizes the results of changing the various parameters about that of the baseline. Major observations are that:

(1) Higher randomization (larger σ_o) increases attenuation vs. frequency of resonances. It is possible even with significant σ_y/dy ratio of of 0.331 to observe a first resonance at

$$f_1 = \frac{c}{2\ dy} \sec \theta_o \qquad (7)$$

(2) As indicated by (7), and Figure 6, the resonances occur at frequencies where down range centroid spacing dy is multiples of projected wavelength $\lambda_o \sec \theta_o$. Larger lookdown angles produce higher resonances.

(3) Increasing the number of illuminated mines in cross range (wider azimuth beamwidth) increases resonant (coherent) return vs. incoherent return. Result is larger S/C enhancement at resonance in proportion to beamwidth (assuming narrow beamwidth).

TABLE 1

FIG. NO	PARAMETER CHANGED	MAJOR EFFECTS
3	$\sigma_o = .01$ m	$\sigma_o \ll \lambda$ over entire freq. range produces highly periodic coherent resonances.
4	Standard Case	$\sigma_y = 0.2$m becomes wavelength comparable yielding rapid decay of coherency with frequency.
5	$\tau = 0.2\,\mu$sec	Doubling the range cell size also doubles (2N + 1) number of mines in coherent function F_c. Results in higher "Q" of response function.
6	$H_o = 1000$m	A lookdown at 45° vis-a-vis near grazing expands freq. scale due to larger projected wavelength. Amplitude increase due to larger range cell projection.
7	$\varphi_B = 10°$	Wider azimuth beamwidth provides larger surface area illumination thus including more mines and increasing amplitude of coherent/ non-coherent return.
8	$\sigma_o = 0.5$m	This causes a very rapid decay of the coherency factor with frequency. The primary resonance at 100 MHz is greatly reduced but still highly visible.

(4) Increasing number of illuminated mines in down range (longer pulse width) increases number of interfering phase centers in the array factor. This produces narrower bandwidth of resonances and sidelobes in frequency and decreases relative sidelobe level thus enhancing observability of resonances in swept frequency mode.

In Figures 9 through 13 the special Class II of a minefield much smaller than the range-azimuth cell of the radar is considered. The plots are of the computed spectra of the array factor rather than the improvement factor

$$F = (1 - e^{-\gamma^2}) F_I + e^{-\gamma^2} F_C \qquad (2a)$$

The standard case is shown in Figure 10

H_o = 100 meters

M_o = 11 Cross range grid size

N_o = 9 Down range grid size

Total No. Mines = 99

σ_o = 0.2 meters

The results are very similar in behavior to that of a large minefield as per resonances and dependence on randomness of mine placement. The S/C improvement factor would have an identical shape to these curves but would be divided by F_I for the entire range-azimuth cell of the radar as given in equation (III-1). The incoherent array factor due to the 99 mines is much larger compared to the coherent factor vis-a-vis the same ratio for the previous set of large mine field results. The first resonance at f_1 (at approximately 20 MHz)

is much less pronounced for even the moderately random case of $\sigma_y = 0.5$ *m* (*Figure* 13); the lower sidelobes of coherent interference dominate the actual first resonance.

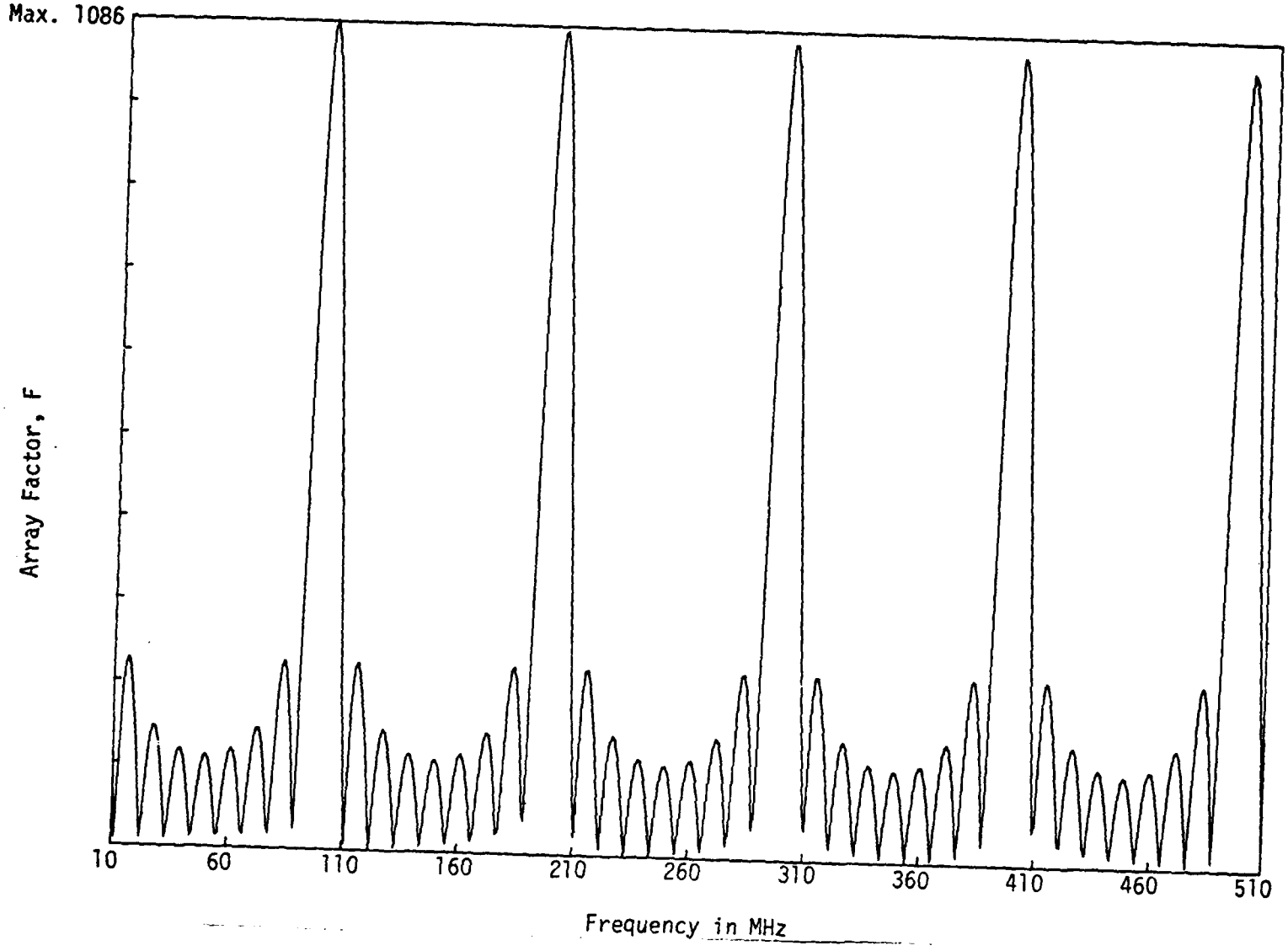

Figure 9. Plot of Class II, F vs. Frequency at same parameters as in Figure 3, except the mine field is finite with 9 rows and 11 columns, i.e., H_o = 100 m, R_1 = 1000 m, ϕ_B = 5°, θ_B = 5°, dx = dy = 1.51 m, $\sigma_o = \sigma_x = \sigma_y$ = .01 m, τ = .1 sec.

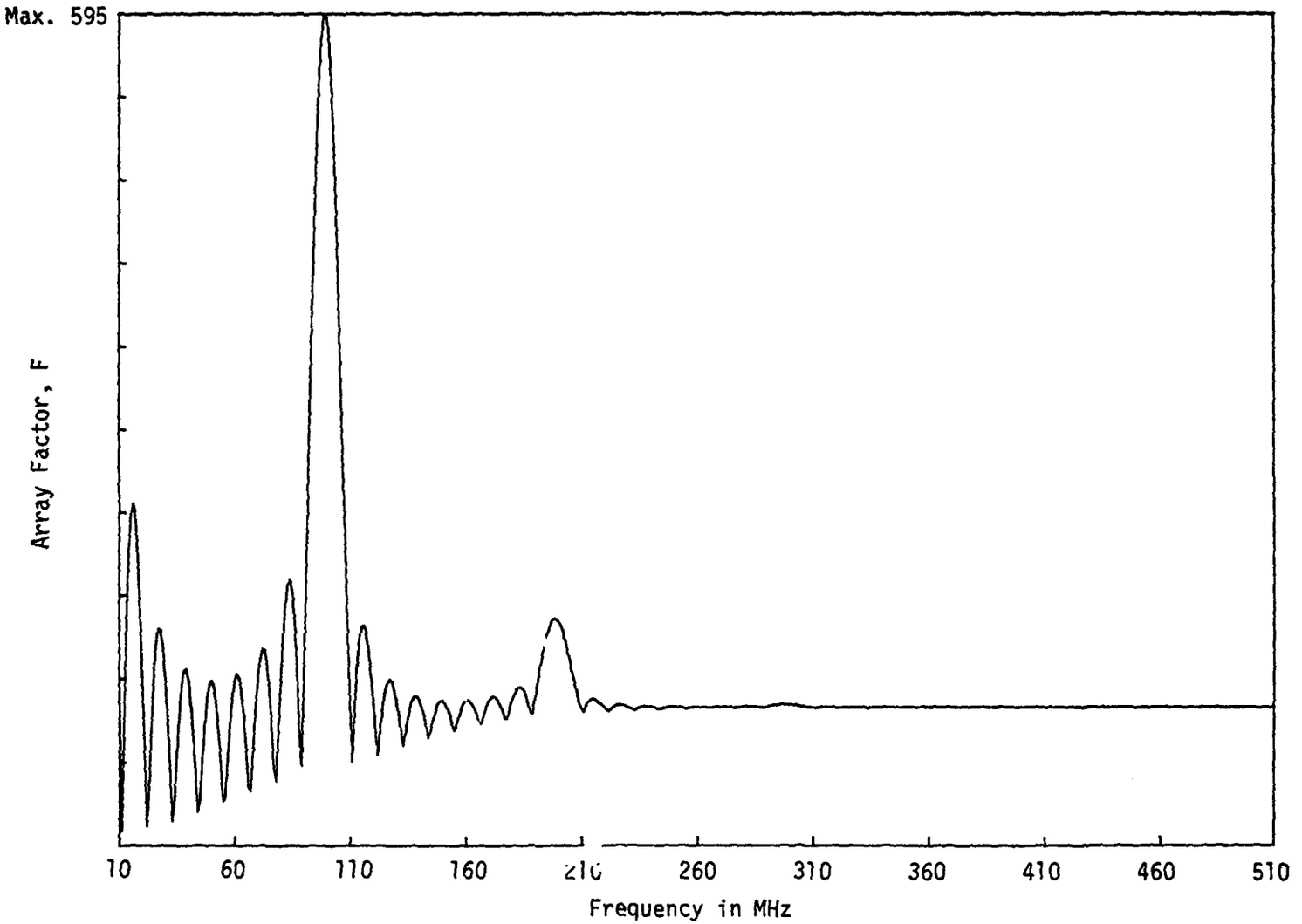

Figure 10. Plot of Class II, F vs. Frequency using same parameters as in Figure 9, except σ_o = .2 m, i.e., H_o = 100 m, R_1 = 1000 m, ϕ_B = 5°, θ_B = 5°, dx = dy = 1.51 m, $\sigma_o = \sigma_x = \sigma_y$ = 0.2 m, τ = .1 μsec.

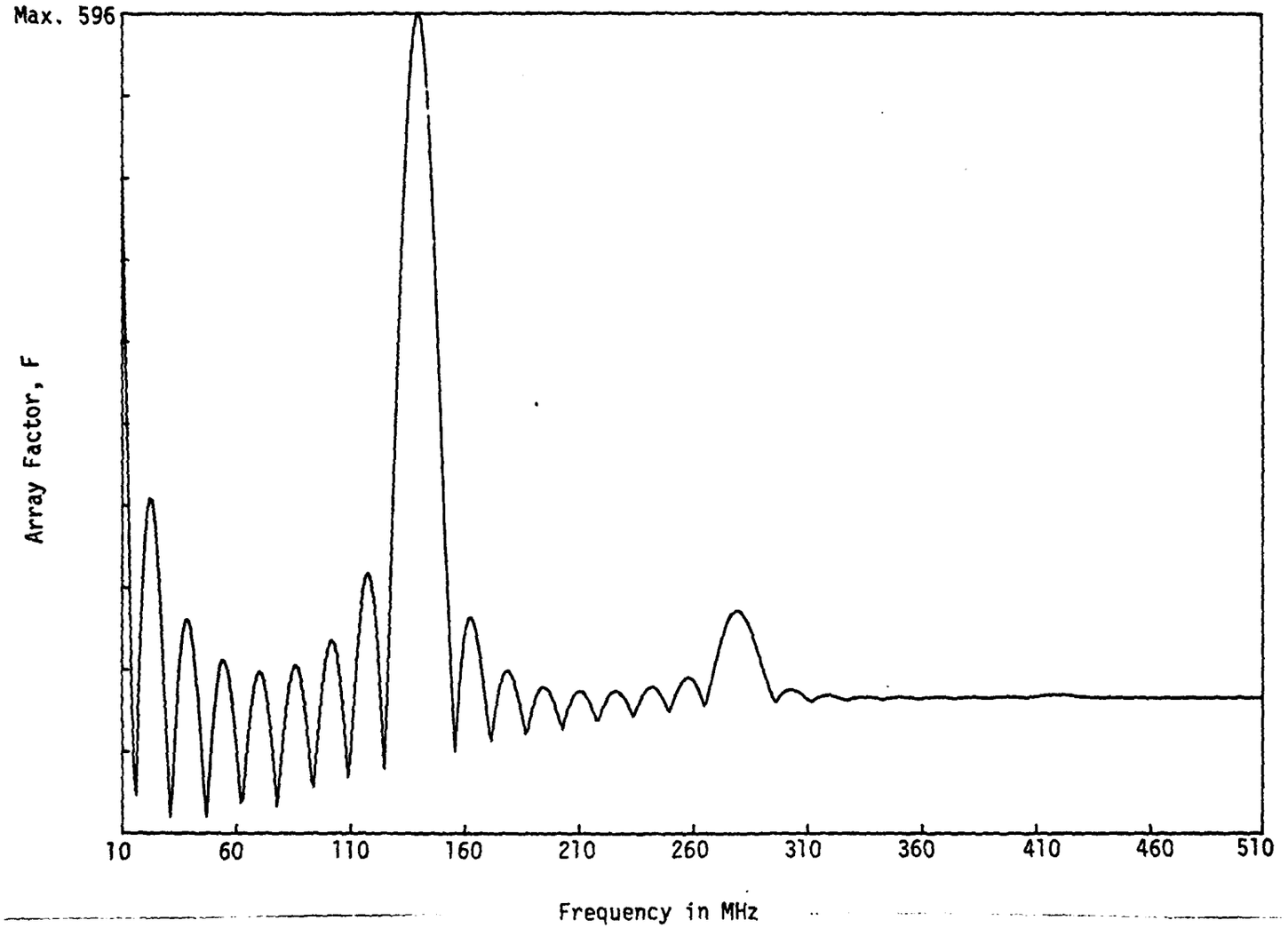

Figure 11. Plot of Class II, F vs. Frequency using same parameters as in Figure 10, except H_o = 1000 m

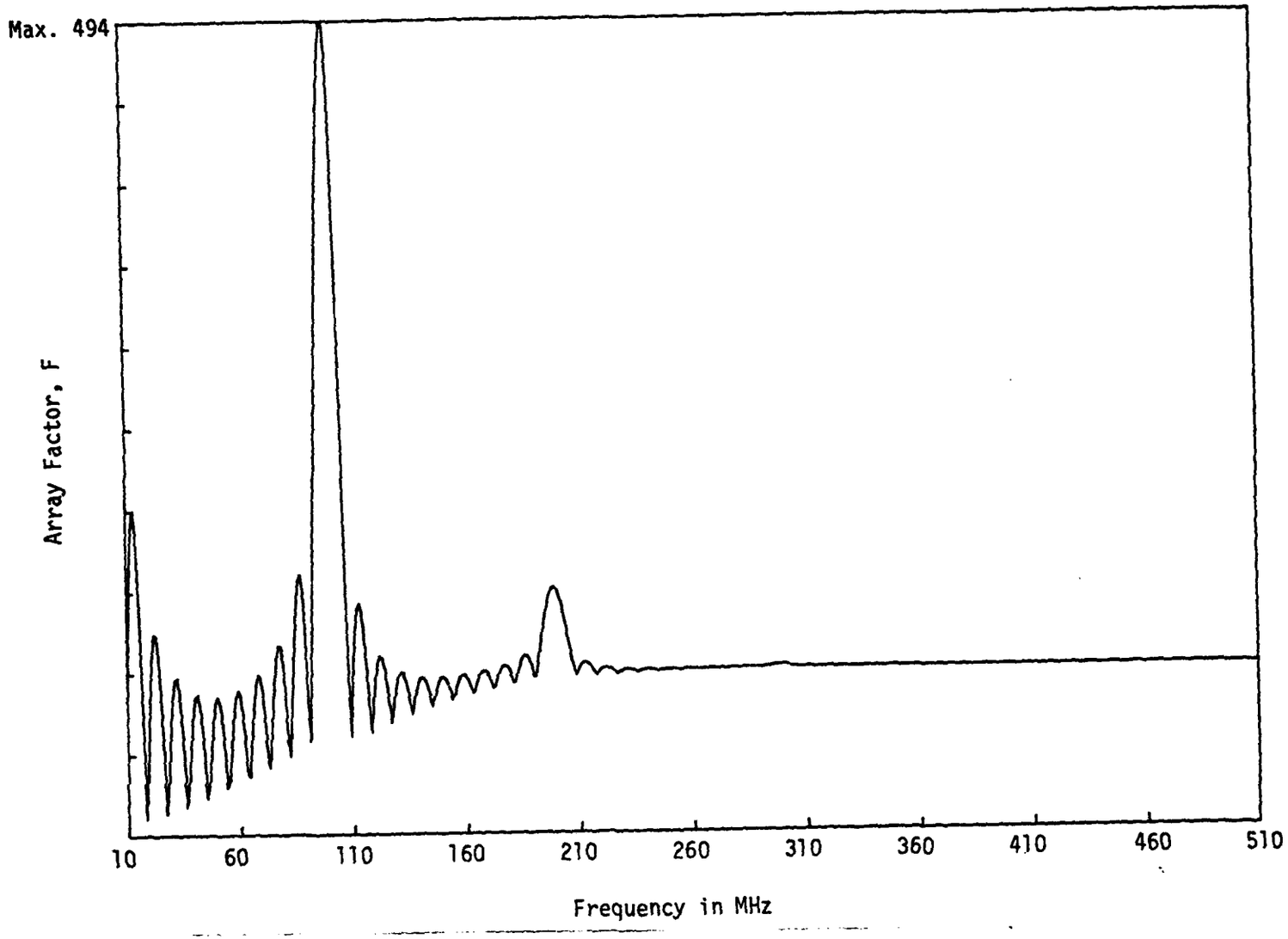

Figure 12. Plot of Class II, F vs. Frequency using same parameters as in Figure 10, except with 11 rows and 9 columns

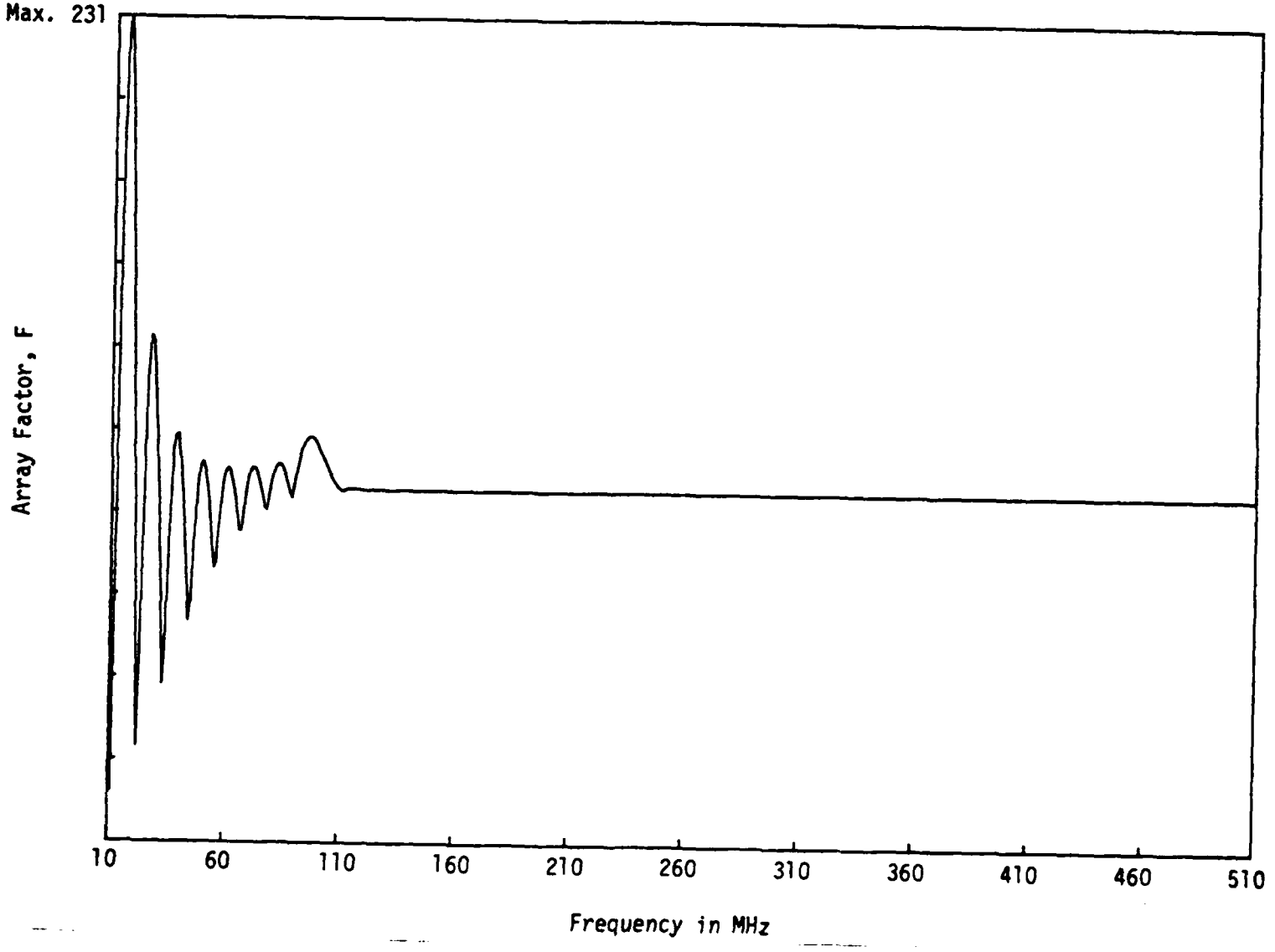

Figure 13. Plot of Class II, F vs. Frequency using same parameters as in Figure 10, except σ_o = 0.5 m

III. METHOD OF ANALYSIS

A. RADAR SCATTERING FUNDAMENTALS

In this section we will briefly review the pertinent equations of electromagnetic scattering that are to be used in the mine field scattering case. Referring to Figure 14, consider a single radar "target" (mine or other object being considered) which is located at a distance of R from the radar which transmits a total peak power of W_t watts into a transmit-receive antenna having gain function $G(\theta,\phi) = G_o B^2(\theta,\phi)$ where G is maximum boresight gain and $B(\theta,\phi)$ is normalized (maximum = unity) field directivity pattern of the antenna. The elevation and azimuth angles off-boresight are θ and ϕ, respectively.

The incident power per unit area at the target location will be [4]

$$p^i = \frac{|\bar{E}^i|^2}{\eta_o} = \frac{W_t\, G(\theta_t,\phi_t)}{4\pi R^2} \tag{8}$$

where $\eta_o = 120\pi$ ohms (free-space wave impedance)

$\bar{E}_i$ = incident electric field phasor (RMS)

θ_t,ϕ_t = target position in gain pattern

Using (8) we solve for the incident electric field magnitude

$$|\bar{E}^i| = \frac{[30\, W_t\, G(\theta_t,\phi_t)]^{1/2}}{R} \tag{9}$$

This can be rewritten in terms of $B(\theta_t,\phi_t)$ and including the relative phase of the incident field phasor in terms of distance, R, and wavenumber, $\beta_o = 2\pi/\lambda_o$, as

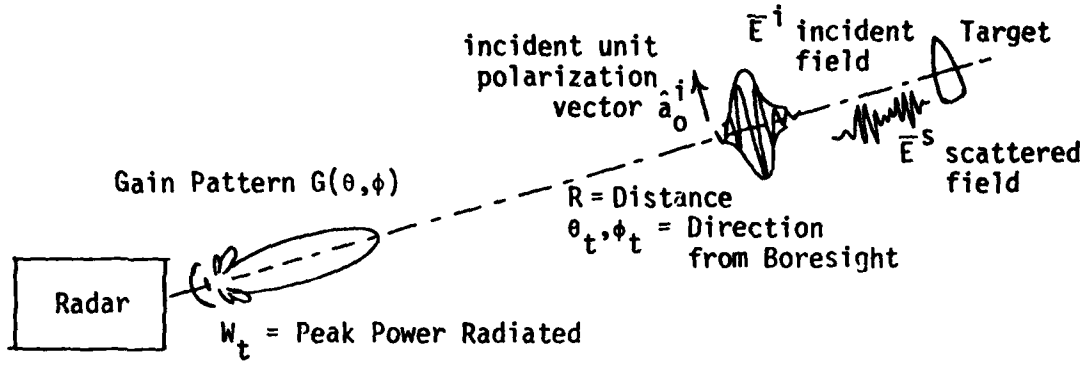

Figure 14. Basic Radar Scattering Parameters

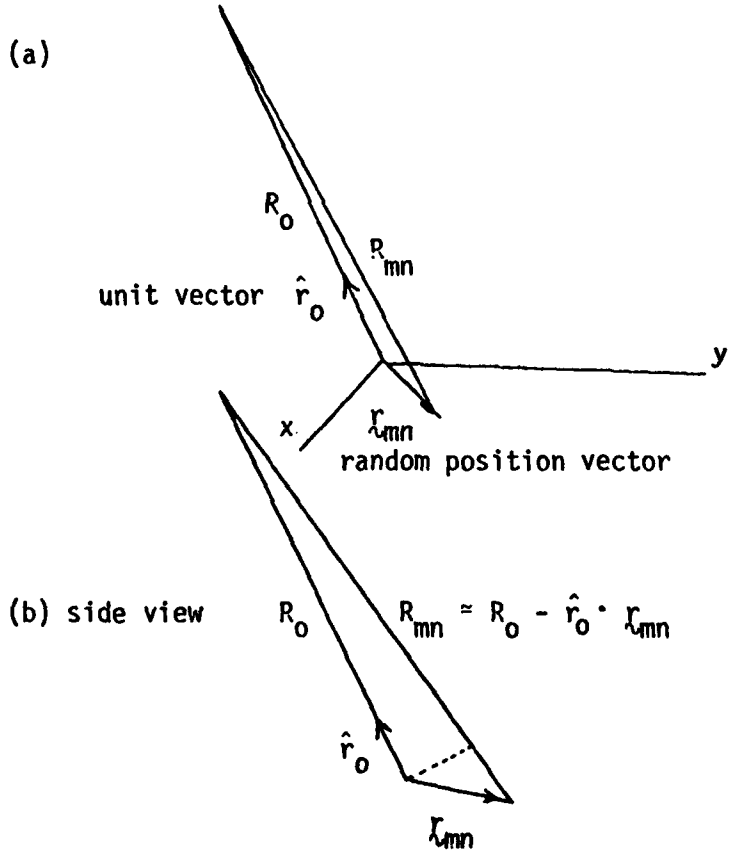

Figure 15. Far-Field Phase Path Length

$$\bar{E}^i = \bar{E}_o \frac{e^{-j\beta_o R}}{R} B(\theta_t, \phi_t) \tag{10a}$$

where

$$\bar{E}_o = (30\, W_t\, G_o)^{1/2}\, \hat{a}_o^i \tag{10b}$$

and

$$B(\theta_t, \phi_t) = \left[\frac{G(\theta_t, \phi_t)}{G_o}\right]^{1/2} \tag{10c}$$

with $\hat{a}_o^i$ the unit polarization vector for the incident $\bar{E}^i$.

The scattering characteristics of the "target" are embodied in its complex scattering matrix, $\underset{\sim}{S}$, which is a 2 × 2 matrix function of incidence angle of illumination for the monostatic (backscattering) case.

$$\underset{\sim}{S} = \begin{bmatrix} S_{VV} & S_{VH} \\ S_{HV} & S_{HH} \end{bmatrix} \tag{11}$$

The complex diagonal elements indicate the amount of self-polarization backscattering while the off-diagonals $S_{VH} = S_{HV}$ (reciprocity derived relationship) indicate the relative cross-polarization effects for a particular aspect on the target. By partitioning the incident electric field phasor into horizontal and vertical components

$$\bar{E}^i = \begin{bmatrix} E_V^i \\ E_H^i \end{bmatrix} \tag{12}$$

The RMS scattered field phasor received at the radar in the "far-field" ($R > \frac{2D^2}{\lambda_o}$, where D = maximum target dimension) is [5]

$$\bar{E}^s = \begin{bmatrix} E_V^s \\ \\ E_H^s \end{bmatrix} = \underset{\sim}{\mathscr{S}} \cdot \bar{E}^i \ \frac{e^{-j\beta_o R}}{R} \tag{13}$$

The complex components of $\underset{\sim}{\mathscr{S}}$ thus indicate relative amplitudes and phases of co-polarization and cross-polarization scattering for a specified aspect. In general $\underset{\sim}{\mathscr{S}}$ has a very complicated behavior of aspect and frequency but can be numerically computed for a range of simple object geometries, although often with great computational effort.

To relate $\underset{\sim}{\mathscr{S}}$ to the usual radar cross section, RCS_o, of the target we note that the power per unit area P^s returned to the radar antenna in the scattered field is [4],

$$P^s = \frac{|\bar{E}^s|^2}{\eta_o} = P^i \frac{RCS_o}{4\pi R^2} \tag{14}$$

Using (8), (13) and (14) yields

$$RCS_o = 4\pi R^2 \frac{|\bar{E}^s|^2}{|\bar{E}^i|^2} = 4\pi \left[\underset{\sim}{\mathscr{S}} \cdot \hat{a}_o^i\right]^2 \tag{15}$$

B. ARRAY FACTOR DERIVATION

Let us now consider the case of backscattering from a random mine field as previously described in Section II and illustrated in Figures 1 and 2. We model the statistical mine field placement by independent random gaussian probability densities with centroid positions at surface locations

$$\bar{r}_{mn} = x_{mn}\,\hat{x} + y_{mn}\,\hat{y}$$

where the double index (m,n) signifies the grid number and $\hat{x}$, $\hat{y}$ are unit vectors in the x and y directions respectively (see Figures 2 and 15). This double index is used for the specific case of a rectangular grid to be used later in summing the coherent and incoherent array

factors, but could just as well be replaced by a global grid number, "k." We will use (m,n) however, noting that the grid arrangement has, per se, no bearing on the expectation calculation.

The S/C calculation proceeds by defining this ratio in terms of time-averages of mine-array and clutter field phasor returns

$$\frac{S}{C} = \frac{\langle \bar{e}_A(t) \cdot \bar{e}_A(t) \rangle}{\langle \bar{e}_C(t) \cdot \bar{e}_C(t) \rangle} = \frac{\langle |\bar{E}_A^S|^2 \rangle}{\langle |\bar{E}_C^S|^2 \rangle} \tag{16}$$

The "A" subscript denotes array while "C" denotes clutter. Assuming that the beam center distance $R_o >> \frac{2L^2}{\lambda_o}$ where L = maximum dimension of the illuminated patch and λ_o = wavelength of the pulse carrier frequency, then the mine and clutter arrays are in the far-field. By assuming simple superposition,

$$\bar{E}_A^S = \sum_m \sum_n \bar{E}_{m,n}^S \tag{17}$$

where $\bar{E}_{m,n}^S$ due to the mine at the random position $\underset{\sim}{r}_{m,n}$ is, from (13),

$$\bar{E}_{m,n}^S = (\bar{\bar{\mathcal{J}}}_{m,n} \cdot \bar{E}_{m,n}^i) \frac{e^{-j\beta_o R_{m,n}}}{R_{m,n}} \tag{18}$$

and $\bar{\bar{\mathcal{J}}}_{m,n} = \bar{\bar{\mathcal{J}}}$ the same scattering matrix for each mine. All mines are assumed identical with the same orientation. Using equation (10), the incident field at the (m,n) mine has the form

$$\bar{E}_{m,n}^i = \bar{E}_o \frac{e^{-j\beta_o R_{m,n}}}{R_{m,n}} B_{m,n} \tag{19}$$

where

$$\bar{E}_o = \left[30\, W_t\, G_o\right]^{1/2} \hat{a}_o^i \tag{20}$$

is the incident field value at the boresight position on the ground ($\bar{r} = 0$) with W_t = Trans Power, G_o = boresight max gain, and $\hat{a}_o^i$ incident unit polarization vector, and

$$B_{mn} = \left[\frac{G_{mn}}{G_o}\right]^{1/2} \tag{21}$$

is the normalized antenna "field gain" at $\bar{r}_{mn}$. The far-field assumption allows replacing $R_{mn} = R_o$ in the denominators of (18) and (19) while the phase terms become $\beta_o R_{mn} \doteq \beta_o(R_o - \hat{r}_o \cdot \bar{r}_{mn})$, as shown in Figure 15. There results

$$\bar{E}_A^S = (\bar{\bar{\mathscr{S}}} \cdot \bar{E}_o) \frac{e^{-j2\beta_o R_o}}{R_o^2} \sum_m \sum_n B_{mn}\, e^{j2\beta_o \hat{r}_o \cdot \bar{r}_{mn}} \tag{22}$$

the signal power becomes

$$\langle |E_A^S|^2 \rangle = \frac{|\bar{\bar{\mathscr{S}}} \cdot \bar{E}_o|^2}{R_o^4} F \tag{23}$$

Using (23) the equivalent radar cross-section of the mine field can be easily found and was given in Section II

$$RCS_M = 4\pi R_o^2 \frac{\langle |\bar{E}_A^S|^2 \rangle}{|E_o^i|^2} = 4\pi |\bar{\bar{\mathscr{S}}} \cdot \hat{a}_o^i|^2 F = RCS_o \cdot F \tag{1}$$

Thus, the average RCS of the random ensemble of identical mines equals the RCS_o of any one mine in the field times an average array factor, F, which is found from (1) and (22) to be the time-average of the sum given by

$$F = \sum_m \sum_n \sum_{m'} \sum_{n'} \left\langle B_{mn}\, B_{m'n'}\, e^{j2\beta_o \hat{r}_o \cdot (\bar{r}_{m,n} - \bar{r}_{m',n'})} \right\rangle \tag{24}$$

The source position direction unit vector is given by

$$\hat{r}_o = \cos\theta_o \cos\phi_o \hat{x} + \cos\theta_o \sin\phi_o \hat{y} + \sin\theta_o \hat{z} \tag{25}$$

while the random mine positions are given by

$$\underset{\sim}{r}_{m,n} = \bar{r}_{m,n} + \sigma_x U \hat{x} + \sigma_y V \hat{y} \qquad \left.\begin{matrix}\sigma_x \\ \sigma_y\end{matrix}\right\} \text{standard deviations} \tag{26}$$

where the joint gaussian probability density is given by, [6],

$$p(u,v) = \frac{1}{2\pi} e^{-(u^2 + v^2)/2} \tag{27}$$

where U and V are independent normalized random variables.
Assuming independence of positions and system ergodicity,

$$F = \sum_m \sum_n \mathcal{E}\left[B_{m,n}^2\right] + \sum_m \sum_n \sum_{m'} \sum_{n'} \mathcal{E}\left[B_{m,n}\, e^{j2\beta_o \hat{r}_o \cdot \underset{\sim}{r}_{m,n}}\right] \tag{28}$$

$$\cdot\, \mathcal{E}\left[B_{m',n'}\, e^{-j2\beta_o \hat{r}_o \cdot \underset{\sim}{r}_{m',n'}}\right]$$

$$m \neq m'$$
$$n \neq n'$$

where

$$\hat{r}_o \cdot \underset{\sim}{r}_{m,n} = \cos\theta_o \cos\phi_o (x_m + \sigma_x U) + \cos\theta_o \sin\phi_o (y_n + \sigma_y V) \tag{29}$$

Assuming that $B_{m,n} = \left[\frac{G_{mn}}{G_o}\right]^{1/2}$ (30)

is essentially constant over several standard deviations in x and y from the centroid of placement of the (m,n) mine then

$$\mathcal{E}\left[B_{m,n}^{\ 2}\right] \doteq B_{m,n}^{\ 2} \tag{31a}$$

and

$$\mathcal{E}\left[B_{m,n}\, e^{\pm j2\beta_o \hat{r}_o \cdot \underset{\sim}{r}_{m,n}}\right] \doteq B_{m,n}\, \mathcal{E}\left[e^{\pm j2\beta_o \hat{r}_o \cdot \underset{\sim}{r}_{m,n}}\right]$$

$$= B_{m,n}\, e^{\pm j2\beta_o \cos\theta_o (\cos\phi_o\, x_m + \sin\phi_o\, y_n)}$$

$$\times \mathcal{E}\left[e^{\pm j2\beta_o \cos\theta_o (\cos\phi_o\, \sigma_x\, U + \sin\phi_o\, \sigma_y\, V)}\right] \tag{31b}$$

To simplify equation (31b) it is convenient to designate the expectation in the last line as $\mathcal{E}$[U and V].

The expectation over x and y (R.V.s U and V) becomes a product of two one-dimensional expectations. Defining

$$\alpha_x = 2\,\beta_o \cos\theta_o \cos\phi_o\, \sigma_x$$
$$\alpha_y = 2\,\beta_o \cos\theta_o \sin\phi_o\, \sigma_y \tag{32}$$

then

$$\mathcal{E}\left[U \text{ and } V\right] = \mathcal{E}\left[\text{on } U\right] \times \mathcal{E}\left[\text{on } V\right] \tag{33a}$$

where

$$\mathcal{E}\left[\text{on } U\right] = \frac{1}{\sqrt{2\pi}} \int_{-\infty}^{\infty} e^{\pm j\alpha_x U}\, e^{-U^2/2}\, dU \tag{33b}$$

Using $\int_0^\infty e^{-a^2x^2} \cos bx\, dx = \frac{\sqrt{\pi}}{2a} e^{-b^2/4a^2}$ $\quad a^2 = 1/2$, $b = \alpha_x$ (34)

yields

$$\mathcal{E}\left[\text{on } U\right] = e^{-\alpha_x^2/2} \tag{35a}$$

Likewise

$$\mathcal{E}\left[\text{on } V\right] = e^{-\alpha_y^2/2} \tag{35b}$$

Thus

$$\mathcal{E}\left[U \text{ and } V\right] = e^{-2\beta_o^2 \cos^2\theta_o(\sigma_x^2 \cos^2\phi_o + \sigma_y^2 \sin^2\phi_o)} \tag{36}$$

Substituting back into (28) yields

$$F = \sum_m \sum_n B_{m,n}^2 \; e^{-4\beta_o^2 \cos^2\theta_o(\sigma_x^2 \cos^2\phi_o + \sigma_y^2 \sin^2\phi_o)}$$

$$\times \sum_m \sum_n \sum_{m'} \sum_{n'} B_{mn} B_{m'n'} e^{j2\beta_o \cos\theta_o\left[\cos\phi_o(x_m - x_m') + \sin\phi_o(y_n - y_n')\right]} \tag{37}$$

$m \neq m'$

$n \neq n'$

Defining

$$\gamma^2 = 4\beta_o^2 \cos^2\theta_o(\sigma_x^2 \cos^2\phi_o + \sigma_y^2 \sin^2\phi_o) \tag{38a}$$

$$\delta_x = 2\beta_o \cos\theta_o \cos\phi_o \tag{38b}$$

$$\delta_y = 2\beta_o \cos\theta_o \sin\phi_o \tag{38c}$$

We can rewrite the total expectation in the form

$$F = (1 - e^{-\gamma^2}) \underbrace{\sum_m \sum_n B_{mn}^2}_{\text{incoherent}} + e^{-\gamma^2} \Big| \underbrace{\sum_m \sum_n B_{m,n} e^{j(\delta_x x_m + \delta_y y_n)}}_{\text{coherent}} \Big|^2 \tag{39}$$

In words,

Array factor = incoherent array factor (additive power) F_I + coherent array factor (additive fields) F_C

This provides our equation (2) from Part II

$$F = (1 - e^{-\gamma})^2 \; F_I + e^{-\gamma^2} \; F_c \qquad (2)$$

and mathematically defines what is meant by F_I and F_c.

In this form the relative amounts of power are clearly shown for the incoherent and coherent factors of the array. As is evident from (39), if $\gamma^2 >> 1$ then the power is essentailly summed incoherently and $F = F_I$. This happens when the projected standard deviation of the mine position is much greater than the wavelength λ_o:

$$\underbrace{(\sigma_x^2 \cos^2\phi_o + \sigma_y \sin^2\phi_o) \cos^2\theta_o}_{\text{Projected Variance of mine position}} >> \underbrace{\lambda_o^2}_{\text{wavelength squared}} \qquad (40)$$

Square of standard deviation

Likewise, if the projected variance is $<< \lambda_o^2$ then the power results from a coherent field summation.

C. ARRAY FACTOR SUMMATIONS

The incoherent and coherent array factor summations can be performed via computer for any specified gain pattern. To obtain approximate results analytically we will model (curve fit) the gain pattern in the main beam to an exponential function of the form

$$G(\theta,\phi) = G_o e^{-a\left|\frac{\theta}{\theta_B}\right|} e^{-a\left|\frac{\phi}{\phi_B}\right|} \qquad (41a)$$

where

θ = elevation (vertical) angle from boresight

ϕ = azimuth (horizontal) angle from boresight

and

θ_B, ϕ_B = 3dB beamwidths

where

$$G(\pm \frac{\theta_B}{2}, 0) = G(0, \pm \frac{\phi_B}{2}) = \frac{1}{2} G_o \tag{41b}$$

which requires that

$$a = 2 \ln 2 = 1.3863 \tag{41c}$$

The absolute value signs in (41a) are put in to make $G(\theta,\phi)$ an even function of θ and ϕ. By assuming that the radar antenna is located in the x = o plane with $\phi_o = -\pi/2$, as shown in Figure 2, will allow an easier evaluation of (39) without any real loss in generality since our coordinate system may be oriented as desired. The modified equations in (38) become

$$\gamma^2 = 4\beta_o^2 \sigma_y^2 \cos^2\theta_o \tag{38'a}$$

$$\delta_x = 0 \tag{38'b}$$

$$\delta_y = -2\beta_o \cos\theta_o \tag{38'c}$$

The projected gain pattern on the surface is obtained by the following approximations for a narrow beam (in azimuth) and short range cell

$$\text{Cross-Range:} \quad |\phi| = \tan^{-1}\left|\frac{x}{R_o}\right| \doteq \left|\frac{x}{R_o}\right| \quad \text{for } \phi_B \text{ small} \tag{42a}$$

$$\text{Range-Projection:} \quad \frac{y}{\sin\theta} = \frac{R_o}{\sin(\theta_o - \theta)} \doteq \frac{R_o}{\sin\theta_o} \quad \text{for } \frac{c\tau}{2} \ll R_o$$

$$\therefore \quad |\theta| \doteq \sin^{-1}\left|\frac{y \sin\theta_o}{R_o}\right| \doteq \left|\frac{y}{R_o}\right| \sin\theta_o \tag{42b}$$

To proceed with the evaluation of F_I and F_C a grid geometry needs to be specified for the centroids of the statistically placed mines. We will assume a rectangular grid arrangement with x and y spacings of d_x and d_y, respectively. The use of a double index (m,n) anticipated this specialization. Equation (39) is equally valid for any specified centroid pattern by replacing (m,n) with single counting index k, with $\sum_m \sum_n \rightarrow \sum_k$ and $(x_m, y_n) \rightarrow (x_k, y_k)$. The use of a rectangular grid (along with the other assumptions made up to this point) will allow an analytic evaluation of F_I and F_C. These expressions will then yield the characteristic type of interactions and trade-offs of parameters that are present for any type of statistical mine configuration being swept by a high resolution radar. As mentioned previously, the case of the entire mine field occupying a small portion of the range-azimuth cell is considered in Appendix II.

Proceeding with the rectangular grid assumption:

$$x_m = m\, d_x \qquad -\infty < m < \infty \tag{43a}$$

$$y_n = n\, d_y \qquad -N < n < N \tag{43b}$$

In performing the summations of F_I and F_C we will limit n by the range cell size

$$N = \text{Integer} \left\{ \frac{c\tau \sec\theta_o}{4\, d_y} \right\} \tag{43c}$$

while m is taken between $\pm\infty$ because the contributions due to non-existent mines beyond the actual mine field will be weighted by the very samll gain factors in (41a) so far off boresight. It is not possible to sum n between $\pm\infty$ because in the cases considered θ_o is small and the values of n with $|n| > N$ would make a significant contribution to the sum. From equations (21), (41a), (42) and (43)

$$B_{mn}^2 = \frac{G_{mn}}{G_o} = e^{-\frac{a}{R_o\phi_B}|x_m|} e^{\frac{-a\sin\theta_o}{R_o\theta_B}|y_n|} \qquad (44)$$

$$= e^{\frac{-ad_x}{R_o\phi_B}|m|} e^{\frac{-ad_y\sin\theta_o}{R_o\theta_B}|n|}$$

substituting into (39) yields

$$F_I = \sum_m \sum_n B_{mn}^2 = \sum_{m=-\infty}^{\infty} e^{\frac{-ad_x}{R_o\phi_B}|m|} \cdot \sum_{n=-N}^{N} e^{\frac{-ad_y\sin\theta_o}{R_o\theta_B}|n|}$$

$$= \sum_{m=-\infty}^{\infty} Z_x^{|m|} \cdot \sum_{n=-N}^{N} Z_y^{|n|} \qquad (45)$$

which is simply the product of two geometric series where

$$Z_x = e^{\frac{-ad_x}{R_o\phi_B}} < 1 \quad \text{and} \quad Z_y = e^{\frac{-ad_y\sin\theta_o}{R_o\theta_B}} < 1 \qquad (45a)$$

These series are easily summed using (I - 1) in Appendix I.

$$\sum_{m=-\infty}^{\infty} Z_x^{|m|} = \frac{1 + Z_x}{1 - Z_x} \quad \text{iff} \quad Z_x < 1 \tag{46a}$$

and

$$\sum_{n=-N}^{N} Z_y^{|n|} = \frac{1 + Z_y - 2Z_y^{(N+1)}}{1 - Z_y} \tag{46b}$$

Using (38'b), (38'c), (43b) and (44) the coherent array factor in (39) is expressible as a product of two geometric series

$$F_c = \left| \sum_m \sum_n B_{mn} e^{j\delta_y y_n} \right|^2$$

$$= \left| \sum_{m=-\infty}^{\infty} e^{\frac{-ad_x}{2R_o\phi_B}|m|} \cdot \sum_{n=-N}^{N} e^{\frac{-ad_y \sin\theta_o}{2R_o\theta_B}|n|} e^{-j2\beta_o d_y \cos\theta_o\, n} \right|^2$$

Using (45')

$$F_c = \left| \sum_{m=-\infty}^{\infty} Z_x^{\frac{|m|}{2}} \cdot \sum_{n=-N}^{N} Z_y^{\frac{|n|}{2}} P^n \right|^2 \tag{47a}$$

where $P = e^{j2\beta_o d_y \cos\theta_o}$ (47b)

Using I-2 in Appendix I we obtain (48a)

$$\sum_{n=-N}^{N} Z_y^{|n|/2} P^n = \{1 - Z_y - Z_y^{(N+1)/2}[P^{N+1} + (1/P)^{N+1}] + Z_y^{(N+2)/2}[P^N + (1/P)^N]\} / \{1 + Z_y - Z_y^{\frac{1}{2}}[P + (1/P)]\}$$

$$= \frac{1 - Z_y - 2(\sqrt{Z_y})^{N+1}\cos[(N+1)2\beta d_y \cos\theta_o] + 2(\sqrt{Z_y})^{N+2}\cos[N2\beta d_y\cos\theta_o]}{1 + Z_y - 2\sqrt{Z_y}\cos(2\beta d_y\cos\theta_o)}$$

While, from (46a) with $Z_x \to Z_x^{\frac{1}{2}}$, yields

$$\sum_{m=-\infty}^{\infty} Z_x^{|m|/2} = \frac{1+\sqrt{Z_x}}{1-\sqrt{Z_x}} \quad \text{iff} \quad Z_x < 1 \tag{48b}$$

The incoherent array factor can be written in terms of hyperbolic trig functions as

$$F_I = \coth\left(\frac{ad_x}{2R_o\phi_B}\right) \coth\left(\frac{ad_y\sin\theta_o}{2R_o\theta_B}\right)\left[1 - \frac{e^{-(N+\frac{1}{2})\left(\frac{ad_y\sin\theta_o}{R_o\theta_B}\right)}}{\cosh\left(\frac{ad_y\sin\theta_o}{2R_o\theta_B}\right)}\right] \tag{49a}$$

while the coherent array factor may be expressed as

$$F_c = \left| \coth\left(\frac{ad_x}{4R_o\phi_B}\right) \right|^2 \tag{49b}$$

$$\times \left| \left\{ \sinh\left(\frac{ad_y \sin\theta_o}{2R_o\theta_B}\right) - \exp\left(-\frac{Nad_y \sin\theta_o}{2R_o\theta_B}\right) \cos[(N+1)2\beta_o d_y \cos\theta_o] \right.\right.$$

$$\left.\left. + \exp\left(-\frac{(N+1)ad_y \sin\theta_o}{2R_o\theta_B}\right) \cos[N2\beta_o d_y \cos\theta_o)] \right\} /$$

$$\left\{ \cosh\left(\frac{ad_y \sin\theta_o}{2R_o\theta_B}\right) - \cos(2\beta_o d_y \cos\theta_o) \right\} \Bigg|^2$$

These expressions may be substituted into (39) to obtain an exact formula for the array factor which is valid under the assumptions of (a) *a large mine field, much larger than the antenna beam*-range cell ground projection, and (b) almost constant gain over several standard deviations $\sqrt{\sigma_x^2 + \sigma_y^2}$ of random position from each centroid in the grid. Certain realistic assumptions may now be made to simplify these formulas. The first of these concerns the results of the infinite x-summations over m. Assuming the gain factor $\exp\left(-\frac{a}{R_o\phi_B}|x|\right)$ changes little in a single centroid step implies that $u = \frac{ad_x}{2R_o\phi_B} << 1$. This allows us to truncate the coth term in (49b) at the first term in the power series $\coth(u) = \frac{1}{u} + \frac{u}{3} - \frac{u^3}{45} + \ldots$ resulting in

$$\coth \frac{ad_x}{2R_o\phi_B} \doteq \frac{2R_o\phi_B}{ad_x} \tag{50}$$

This same result is obtained by approximating the m-series in (45) and (47a) by continuous integrals over $-\infty < x < \infty$. The validity of this integral approximation is also contingent upon the small change of the integrand with step size in the original sum.

Additional simplifications result by considering two special, but realistic, cases of practical interest. These cases result by considering the behavior of the y-projected gain pattern over the range-cell length set by the radar pulse width and depression angle. The gain pattern y-projection has the form $\exp\left(-\frac{\sin\theta_o}{R_o\phi_B}\ |y|\right)$ where the range-cell has

$$|y| \leq \frac{c\tau}{4}\ \sec\theta_o.$$

Consider two cases:

Case I

$\frac{c\tau\tan\theta_o}{4R_o\theta_B} << 1$ implies that the gain is approx. constant within the range cell $Z_y \doteq 1$ and $Z_y^N \doteq 1$.

thus $\sum_{n=-N}^{N} Z_y^{|n|} \doteq 2N + 1$ and the incoherent array factor becomes

$$F_I \doteq (2N + 1)\ \frac{2R_o\phi_B}{ad_x} \qquad (51a)$$

while the Z_y sum in F_c becomes that for a uniform array

$$\sum_{n=-N}^{N} Z_y^{|n|/2} P^n \doteq \sum_{n=-N}^{N} P^n = \frac{\sin[(2N+1)\beta_o d_y \cos\theta_o]}{\sin(\beta_o d_y \cos\theta_o)} \tag{51b}$$

yielding

$$F_c \doteq \left(\frac{4 R_o \phi_B}{a d_x}\right)^2 \left|\frac{\sin[(2N+1)\beta_o d_y \cos\theta_o]}{\sin(\beta_o d_y \cos\theta_o)}\right|^2 \tag{51c}$$

This case will, in most applications, be the most commonly occurring in a surface search mode of operation, with exceptions occurring only at the closest ranges having nearly straight down depression angles.

Case II

$\frac{c\tau \tan\theta_o}{4 R_o \theta_B} >> 1$ implies that the range-cell due to pulse width is much larger than the elevation beamwidth projected gain pattern. In this case we may extend N to $\pm\infty$ in the n-series for the same reason that the m-series was extended to $\pm\infty$. The end result of this is that exponential terms in (49a) (49b) with neg. arguments containing the N multiplicative factor may be considered to be vanishingly small. In addition, we may approximate the hyperbolic functions having small arguments, $u << 1$, by the first terms in their power series:

$\coth u \doteq \frac{1}{u}$, $\sinh u \doteq u$, $\cosh u \doteq 1 + \frac{u^2}{2}$ yielding

$$F_I \doteq \frac{4 R_o^2 \theta_B \phi_B}{a^2 d_x d_y \sin\theta_o} \tag{52a}$$

$$F_c \doteq \left(\frac{4 R_o \phi_B}{a d_x}\right)^2 \cdot \left| \frac{\left(\frac{a d_y \sin\theta_o}{2 R_o \theta_B}\right)}{1+\frac{1}{2}\left(\frac{a d_y \sin\theta_o}{2 R_o \theta_B}\right)^2 - \cos(2 \beta_o d_y \sin\theta)} \right|^2 \tag{52b}$$

We are now in a position to complete the formulation of the problem, which, restated, is to investigate optimum radar parameters for enhancing the signal to clutter power ratio in scanning the mine field. This brings up the topic of clutter.

D. SIGNAL TO CLUTTER RATIO

The clutter return is, by definition, due to all undesirable scatterers being illuminated by the radar. Those clutter scatterers which are colocated with the target in the same range/cross range cell will provide an echo signal which will tend to mask the target. In the case being considered of an airborne surface-search radar, the clutter echoes will be due to scattering by the illuminated ground surface patch (even if the surface were flat and smooth) plus scattering by any or all individual scatterers such as rocks, boulders, vegetation (including grass and trees), buildings and other constructed objects. The amounts of scattering by the ground surface alone will depend upon the grazing angle, frequency and degree of surface roughness, [3].

The analysis of total average clutter echo power is similar to that performed for the case of random mine placement. The surface is modelled by an ensemble of totally random scatterers which represent the undulations of the surface, as well as grass, rocks, etc. The assumption of incoherent power addition is usually made. This assumption is valid when the standard deviations of the positions of the scatterers are much greater than one wavelength. This assumption is equivalent to setting $\gamma = \infty$ in (39) which makes $F = F_I$.

This assumption of incoherence is usually a valid approximation except in special cases where some periodic or regular structure is present in the surface clutter ensemble. Examples would be a plowed field or wire fence or row of planted trees. The coherent echoes would be enhanced at frequencies where phase addition or subtractions occur--usually at periodic spacings which are multiples of a projected half-wavelength.

We will assume that clutter is due to an incoherent ensemble of surface scatterers which are randomly distributed about the range-azimuth cell of the radar in a homogeneous manner. By defining a continuous average cross section per unit surface area for the clutter scatterers we can use (1) in conjunction with (39) where $F = F_I(\gamma \to \infty)$ to obtain an equivalent clutter cross section in the range-azimuth cell.

$$RCS_C = RCS'_C \int\int_{\text{surface cell}} B^2(x,y)\, dx\, dy \tag{53}$$

where RCS'_C = clutter cross section per unit area, which is assumed to be constant, and $B^2(x,y) = G(x,y)/G_o$ = normalized antenna power gain.

Using the projected gain pattern from (41a), (42a) and (42b) and assuming the range-cell projection is less than the beam width elevation projection (see Figure 1b) and that we make negligible error in extending the x integral to infinity

$$RCS_C = RCS'_C \int_{-\infty}^{\infty} \int_{-\frac{c\tau}{4}\sec\theta_o}^{+\frac{c\tau}{4}\sec\theta_o} e^{-\frac{a}{\phi_B R_o}|x|} e^{-\frac{a \sin\theta_o}{\theta_B R_o}|y|}\, dy\, dx$$

$$= \frac{4\, RCS'_C\, R_o^2\, \theta_B\, \phi_B}{a^2 \sin\theta_o}\left[1 - e^{-\frac{ac\tau \tan\theta_o}{4 R_o \theta_B}}\right] \tag{54}$$

This result can be simplified under the special conditions of Cases I and II previously considered.

<u>Case I</u> $\frac{c \tan_o}{4 R_o \theta_B} << 1$ Gain constant in Range Cell

We replace $e^{-u} \doteq 1 - u$ in (54) yielding

$$RCS_C \doteq RCS'_C \frac{R_o \phi_B c\tau \operatorname{Sec} \theta_o}{a} \tag{55}$$

As mentioned, this is the case most often encountered.

Case II $\frac{c\tau \tan \theta_o}{4 R_o \theta_B} >> 1$ Projected range-cell is large enough that gain falls to nearly zero at ends of range cell. Here we ignore e^{-u} in (54), yielding

$$RCS_C \doteq RCS'_C \frac{4 R_o^2 \theta_B \phi_B}{a^2 \sin \theta_o} \tag{56}$$

The signal to clutter ratio is easily obtained by noting that the echo returns from both the mine field and clutter may be written in terms of their respective cross sections by

$$W_r = W_t \frac{G_o^2 \lambda_o^2 \cdot (RCS)}{(4\pi)^3 R_o^4} \quad \text{Echo Power at Receive Antenna Output} \tag{57}$$

where W_t = transmitted power and λ_o = wavelength. In taking the ratio (S/C) all terms cancel except the cross sections leaving our original equation (3) in part II

$$\frac{S}{C} = \frac{RCS_M}{RCS_C} \tag{3}$$

The general formula for this ratio is obtained via (1), (39), (49) and (54) and is computed using a computer program described in Appendix III.

Rather than iterating the radar parameters blindly to optimize S/C in the computer program for a given case of mine field statistics let us step back for a moment to look at some generic observations and conclusions.

E. GENERAL CONCLUSIONS

Our task is to select an optimum illumination angle and radar frequency so as to maximize the signal echo from the mine field while minimizing (or at least not maximizing) the clutter echo power. Using (1), (2), (3) and (54) the ratio we wish to maximize is

$$\left(\frac{S}{C}\right) = \frac{RCS_o}{RCS'_C} \times \frac{(1 - e^{-\gamma^2})\, F_I + e^{-\gamma^2} F_C}{A_e} \tag{58}$$

where

$$A_e = \frac{4 R_o^2 \theta_B \phi_B}{a^2 \sin \theta_o}\left[1 - e^{-\frac{ac\tau \tan \theta_o}{4 R_o \theta_B}}\right]$$

is the equivalent gain-weighted surface area for incoherent clutter echo. In (39) the summation $F_I = \sum\sum B_{mn}^2$ can also be expressed approximately in terms of A_e by replacing the summation by an integral as in (54).

$$F_I \doteq \frac{1}{\Delta x\, \Delta y} \iint_{\substack{\text{illuminated} \\ \text{patch}}} B^2(x,y)\, dx\, dy \tag{59}$$

where $\Delta x = d_x$ and $\Delta y = d_y$ are the mine centroid spacings

$$F_I \doteq \frac{A_e}{d_x d_y} = \frac{\text{weighted illuminated area}}{\text{patch area per mine}} \tag{60}$$

This same result is obtained from (49a) when $\frac{ad_x}{2 R_o \phi_B} << 1$, and

$$\frac{ad_y \sin \theta_o}{2 R_o \theta_B} << 1 \quad \text{and} \quad -(N + 1/2)\frac{ad_y \sin \theta_o}{R_o \theta_B} \doteq \frac{-ac\tau \tan \theta_o}{4 R_o \theta_B} \tag{61}$$

which is valid for large N and small changes of $B^2(x,y)$ in advancing one Δx or Δy.

Dividing numerator and denominator of (58) by F_I and using (60), we obtain the result discussed in Section II,

$$\frac{S}{C} \doteq \frac{RCS_o}{d_x\, d_y\, RCS_C} \times \left\{ (1 - e^{-\gamma^2}) + e^{-\gamma^2}\, \frac{F_C}{F_I} \right\} \tag{4}$$

$$= \underbrace{\frac{RCS_o}{d_x\, d_y\, RCS_C}}_{\text{ratio of mine cross section per unit surface area to clutter cross section per unit area}} \times \left\{ 1 + e^{-\gamma^2} \left(\frac{F_C}{F_I} - 1 \right) \right\}$$

This is a very useful result from which to approach the optimization of (S/C). The outside multiplicative term is simply the ratio of mine and clutter cross section densities. This ratio will depend upon mine geometry, mine orientation, polarization, frequency and number of mine per unit area as well as type of clutter present. Unless the individual mines are excited at a resonant frequency of the individual mine cross section RCS_o this ratio will probably be small. This is one approach which should be investigated since the frequencies for resonant RCS_o of a typical mine will be in the GHz regime. Another approach is to optimize the apparent cross section improvement factor I, in the curly brackets. This will be done by first choosing a frequency so that

$$\gamma^2 = 4\, \beta_o^2\, \sigma_y^2\, \cos^2 \theta_o << 1 \tag{62}$$

This requires a frequency low enough that the projected wavelength is much greater than the standard deviation of the random mine placements in the grid: $\lambda_o/\cos\theta_o >> \sigma_y$. Since σ_y could be several meters to several dozen meters this could require relatively low frequencies for normal radar operation (in the VHF or even HF regions) or a look down angle that is nearly vertical

($\theta_o \to 90°$). In this latter case the clutter cross section RCS'_C will generally rise due to partial coherence of the surface scatterers, [3].

Assuming $\gamma^2 << 1$ then the frequency and aspect angle must be chosen to increase $F_C >> F_I$. This can be done by selecting

$$\beta_o d_y \cos \theta_o = n\pi \qquad (n = \text{integer}) \tag{63}$$

so there is phase coherence between the echoes of the centroid positions. The simultaneous solutions of (62) and (63) will only be possible if

$$\frac{\sigma_y}{d_y} << \frac{1}{2n\pi} \tag{64}$$

ideally--say $\frac{\sigma_y}{d_y} \leq \frac{1}{4\pi}$ for instance. This restriction states physically that the randomization (σ_y) of the grid should be much smaller than the average grid spacing. This ratio indicates how random the mine placement is. If the grid is too random then $F \doteq F_I$ and we are stuck with trying to resonate the echoes from individual mine scatterers.

APPENDIX I. SUMMATION FORMULAE

The summations to be performed are of the forms

$$\sum_{k=k_1}^{k_2} z^{|k|} = \frac{1}{1-z} \begin{cases} z^{k_1} - z^{(k_2+1)} & k_2 > k_1 \geq 0 \\ 1 + z - z^{|k_1|+1} - z^{(k_2+1)} & k_2 \geq 0 > k_1 \\ z^{|k_2|} - z^{|k_1|+1} & 0 > k_2 > k_1 \end{cases} \tag{I-1}$$

$$\sum_{k=k_1}^{k_2} z^{|k|} Z^k = \begin{cases} \dfrac{(zZ)^{k_1} - (zZ)^{k_2+1}}{1-(zZ)} & k_2 > k_1 \geq 0 \\ \dfrac{(z/Z)[1-(z/Z)^{|k_1|}]}{1-(z/Z)} + \dfrac{1-(zZ)^{k_2+1}}{1-(zZ)} & k_2 \geq 0 > k_1 \\ \dfrac{(z/Z)^{|k_2|} - (z/Z)^{|k_1|+1}}{1-(z/Z)} & 0 > k_2 > k_1 \end{cases} \tag{I-2}$$

APPEND X II. SCATTERING FACTORS FOR SMALL MINE FIELDS

For the case of a mine field which occupies only a small portion of the surface projected area of the radar range-azimuth cell certain modifications need to be made in evaluating F_I and F_C for insertion into (39) and (58). This special case could occur when a wide beamwidth, long ranges, or small mine field areas are encountered.

The assumption here is that the gain value on all illuminated mines is essentially constant with $B_{m,n}^2 = B_o^2 \leq 1$ depending upon the mine field position in the beam. From (39) we then have

$$F_I = \sum_m \sum_n B_{mn}^2 = B_o^2 \underbrace{(2M + 1)(2N + 1)}_{\text{total \# mines}} \tag{II-1}$$

From (38'), (39) and (43)

$$F_C = \left| \sum_m \sum_n B_{mn} e^{-jn2\beta_o d_y \cos\theta_o} \right|^2$$

$$= (2M + 1)^2 B_o^2 \left| \sum_{n=-N}^{N} p^n \right|^2 \tag{II-2}$$

where

$$p = e^{j2\beta_o d_y \cos\theta_o} \tag{II-3}$$

The geometric series in (II-2) provides a result which is identical to that of the array factor for a uniform linear array with element spacing of 2 d_y. (See (47b) and (51b)).

$$F_C = (2M + 1)^2 \, B_o^2 \left| \frac{\sin[(2N+1)\beta_o d_y \cos\theta_o]}{\sin[\beta_o d_y \cos\theta_o]} \right|^2 \qquad \text{(II-4)}$$

When the dimension $(2N + 1)\, d_y >> \lambda_o$ this coherent array factor will be a very rapidly changing function of θ_o. This array factor will have a lobe structure with

$$F_{C_{max}} = (2M + 1)^2 \, (2N + 1)^2 \, B_o^2 \qquad \text{(II-5)}$$

when

$$\theta_o = \cos^{-1}\left[\frac{n\,\lambda}{2d_y}\right]$$

and $2N - 1$ secondary maxima about 13.5 dB below $F_{C_{max}}$ and approximately equispaced in θ_o between global maxima. There are also 2N nulls located between each $F_{C_{max}}$ angle - again with approximately equal spacing.

The lobe structure in F_C will be very fine for a mine field dimension $(2N + 1)\, d_y >> \lambda_o$ with angles between nulls of

$$\Delta\theta_{null} \approx \sqrt{\frac{\lambda}{2N\, d_y}} \text{ radians} \qquad \text{(II-6)}$$

For Example: f = 10 GHz and $2N\, d_y$ = 20 meters (range dimension of mine field)

yields $\Delta\theta_{null} \approx \sqrt{\frac{3 \text{ cm}}{200 \text{ cm}}} = .039 \text{ rad} \approx 2.2°$ (spacing between nulls)

APPENDIX III. COMPUTER PROGRAMS

Case I. Programming (S/C) Using Equation (58)

Using (59) which assumes that

$$F_I \doteq \frac{1}{d_x d_y} \iint_{\substack{\text{illuminated} \\ \text{patch}}} B^2(x,y)\ d_x d_y \tag{III-1}$$

$$= \frac{4R_o^2 \theta_B \phi_B}{d_x d_y a^2 \sin\theta_o} \left[1 - e^{-\frac{ac\tau\tan\theta_o}{4R_o\theta_B}}\right] .$$

The replacement of the $\sum\sum$ assumes that $B^2(x,y)$ has small changes from one mine centroid to the next and that the mine field extends far beyond the beamwidth in the transverse direction yielding $-\infty < m < \infty$. Using this same assumption the coherent array factor summation in m can be converted to an integral. The result of this is obtained by the approximation in (51c)

$$F_c \doteq \left(\frac{4R_o\ \phi_B}{ad_x}\right)^2 \left|\frac{\sin\ (2N + 1)\ \beta_o d_y\ \cos\theta_o}{\sin\ (\beta_o dy\ \cos\theta_o)}\right|^2 \tag{III-2}$$

where $(2N + 1)$ = Integer Part of $\dfrac{c\tau\ \sec\theta_o}{2\ d_y}$

= No. of mines within the pulse range resolution in the y-direction

This approx. also assumes that the gain does not change significantly as a function of range within the range-cell projection:

$$\frac{c\tau \tan\theta_o}{4R_o\theta_B} << 1 \qquad \text{Assuming low grazing angles} \qquad \text{(III-3)}$$

The equation to be programmed is (4) in Section III-E

$$(S/C) = \frac{RCS_o}{d_x d_y RCS_C} \left\{ 1 + e^{-\gamma^2 \left[\frac{F_c}{F_I} - 1 \right]} \right\} \qquad \text{(III-4)}$$

mine to clutter
cross section density ratio

where $\gamma = 2\beta_o \sigma_y \cos\theta_o$ (III-5)

The resultant computer code as programmed in BASIC for use on an HP-85 microcomputer is shown in Figure III-1. Input parameters as requested by the program are:

Platform Height (meters)

Ground distance to Main Beam Control

Vertical and Horizontal Beamwidths
in Degrees

ΔX (cross range) and ΔY (down range)
grid centroid spacings in meter

Figure III-1 BASIC Computer Program
Large Mine Field Case

```
 10 OPTION BASE 1
 20 DIM F$(1000)
 30 DISP "ENTER MGT * GPE D1 * D
    "
 35 !INTEGER MA
 40 INPUT MP,R1
 50 PRINT "P0=",M0
 60 PRINT "P1=",R1
 70 S0=SQR(M0^2+R1^2)
 80 DISP "ENTER FLSRD BNNID(.02E0
    "
 90 INPUT T0,P0
100 PRINT "T0=",T0
110 PRINT "P0=",P0
120 T0=PI*T0/180
130 P0=PI*P0/180
140 DISP "ENTER DX & DY GRID(M)"
150 INPUT D1,D2
160 PRINT "DX=",D1
170 PRINT "DY=",D2
180 DISP "ENTER SIGMA-Y (M)"
190 INPUT D3
200 PRINT "SIGMA-Y=",D3
210 DISP "ENTER PULSE WID(USEC)"
220 INPUT T1
230 PRINT "PULSE WIDTH(USEC)=",T
    1
240 C0=300*T1
250 P0=2*LOG(2)
260 DISP "ENTER FSRT,FSTOP(GHZ)"
270 INPUT F5,F6
280 PRINT "FSTART(GHZ)=",F5
290 PRINT "FSTOP (GHZ)=",F6
300 DISP "ENTER NO DATA POINTS"
310 DISP "N<=1000"
320 INPUT N
330 PRINT "NO DATA POINTS=",N
335 REDIM F7(N)
340 F7=(F6-F5)/(N-1)
350 PRINT "FREQ INTRVL(GHZ)=",F7
360 N6=C0*R0/(2*D2*R1)
370 FOR I=1 TO N
380 F0=F5+(I-1)*F7
390 B0=20*PI*F0/3
400 G0=(2*B0*D3*R1/R0)^2
410 IF G0<1000 THEN 440
420 C1=0
430 GOTO 450
440 C1=EXP(-G0)
450 O0=4*P0*P0.(A0*D1)
460 A2=A0*C0*H0/(4*R0*T0*P1)
470 F1=O0*T0*P0^2/(A0*D2*H0)
480 F1=F1*(1-EXP(-A2))
485 B4=B0*D2*R1/F0
490 A3=ABS(SIN(N6*B4))
500 A4=ABS(SIN(B4))
510 IF A4>.00000001 THEN 540
520 S1=C0*P0/(2*D2*R1)
530 GOTO 550
540 S1=A3/A4
550 F2=(00*S1)^2
560 F2(I)=1+C1*(F2/F1-1)
580 NEXT I
590 DISP "CALCULATIONS COMPLETE"
593 M1=AMAX(F3)
594 I1=AMAXROW
595 F8=F5+(I1-1)*F7
596 PRINT "MAX S/C=",M1
597 PRINT "FMAX(GHZ)=",
600 DISP "WHEN PLOTTER IS READY"
610 DISP "ENTER LINETYPE 1 TO 4"
620 INPUT L0
640 PLOTTER IS 705
650 FRAME
660 SCALE 1,N,0,M1
670 XAXIS 0,N/10,1,N
680 YAXIS 0,M1/10,0,M1
690 MOVE 1,0
700 LINETYPE L0
710 FOR I=1 TO N
720 PLOT I,F3(I)
730 NEXT I
740 PENUP
750 END
```

Case II. Special Case Program - Uniform Illumination

The total Array Factor, from (39) and (38'a), is

$$F = (1 - e^{-\gamma^2})\ F_I + e^{-\gamma^2}\ F_c \qquad \text{(III-7)}$$

where $$\gamma^2 = 4\beta_o^2\sigma_y^2\cos^2\theta_o \qquad \text{(III-8)}$$

is the coherency factor with σ_y the std. deviation

Assuming $$B_{m,n} = \left[\frac{G_{m,n}}{G_o}\right]^{\frac{1}{2}} = 1 \quad \text{all m,n} \qquad \text{(III-9)}$$

for the case of uniform boresight illumination we have from (II-1)

$$F_I = (2M+1)\cdot(2N+1) \text{ total No. of Mines}$$

where $2M+1$ cross range columns, $2N+1$ = down range rows and (II-4)

$$F_C = (2M+1)^2 \left|\frac{\sin\{(2N+1)\beta_o d_y \cos\theta_o\}}{\sin(\beta_o d_y \cos\theta_o)}\right|^2 \qquad \text{(III-10)}$$

The equivalent RCS of the array is from (1)

$$RCS_M = RCS_o \; F \qquad \text{(III-11)}$$

assuming uniform mine shapes, composition & orientations

The programming of F from (III-7) for this special case of uniform illumination (Appendix II) results in the BASIC code shown in Figure III-2. This code is a modified version of that in Figure III-1 with inputs:

Platform Height and Ground Distance

Cross Range Number of Columns in the Basic Mine Grid

Down Range Number of Rows

ΔX, ΔY Grid Centroid Spacings

σ_y (Standard Deviation)

Start and Stop Frequencies (GHz)

No. of Frequency Points

Output:

$F3(I) = (1 - e^{-\gamma^2})\; F_I + e^{-\gamma^2}\; F_c$ = F "improvement factor"

for $F5 \leq f \leq F6$

Figure III-2 BASIC Computer Program
Small Mine Field Case

```
10 REM SPECIAL UNIFORM ILLUMI
11 REM PROGRAM 4/20/82
12 OPTION BASE 1
20 DIM F3(1000)
30 DISP "ENTER HGT & GRD DIS(M)
   "
40 INPUT H0,R1
50 PRINT "H0=",H0
60 PRINT "R1=",R1
70 R0=SQR(H0^2+R1^2)
80 DISP "ENTER CROSS RNG COL N0
   "
90 INPUT N0
100 DISP "ENTER DOWN RNG ROW N0"
110 INPUT N0
120 PRINT "CRS RNG COL N0=",N0
130 PRINT "DWN RNG ROW N0=",N0
135 F1=M0*N0
140 DISP "ENTER DX & DY GRID(M)"
150 INPUT D1,D2
160 PRINT "DX=" D1
170 PRINT "DY=",D2
180 DISP "ENTER SIGMA-Y (M)"
190 INPUT D7
200 PRINT "SIGMA-Y=",D3
240 DISP "ENTER FSTART,FSTOP(GHZ)"
270 INPUT F5,F6
280 PRINT "FSTART(GHZ)=" F5
290 PRINT "FSTOP (GHZ)=",F6
300 DISP "ENTER NO. DATA POINTS"
310 DISP "N<=1000"
320 INPUT N
330 PRINT "NO DATA POINTS=",N
335 REDIM F7(N)
340 F7=(F6-F5)/(N-1)
350 PRINT "FREQ INTRVL(GHZ)=",F7
370 FOR I=1 TO N
380 F0=F5+(I-1)*F7
390 B0=20*PI*F0/3
400 G0=(2*B0*D3*R1/R0)^2
410 IF G0<1000 THEN 440
420 C1=0
430 GOTO 490
440 C1=EXP(-G0)
490 A2=ABS(SIN(N0*B0*D2*R1/R0))
500 A4=ABS(SIN(B0*D2*R1/R0))
510 IF A4> .00000001 THEN 540
520 F2=F1*F1
530 GOTO 550
540 F2=M0*M0*A2/A4
550 F3(I)=(1-C1)*F1+C1*F2
580 NEXT I
590 DISP "CALCULATIONS COMPLETE"
593 M1=AMAX(F3)
594 C1=AMAXPOW
595 F9=F5+(C1-1)*F7
596 PRINT "MAX F=",M1
597 PRINT "FMAX(GHZ)=",F9
600 DISP "WHEN PLOTTER IS READY"
610 DISP "ENTER LINETYPE 1 TO 4"
630 INPUT L0
640 PLOTTER IS 705
650 FRAME
660 SCALE 1,N,0,M1
670 XAXIS 0,N/10,1,N
680 YAXIS 0,M1/10,0,M1
690 MOVE 1,0
700 LINETYPE L0
710 FOR I=1 TO N
720 PLOT I,F3(I)
730 NEXT I
740 PENUP
750 END
```

REFERENCES

[1] M.I. Skolnik, Introduction to Radar Systems, 2nd Ed., McGraw-Hill, New York, 1980.

[2] A. Ishimaru, Wave Propagation and Scattering in Random Media, Academic Press, New York, 1978.

[3] D.K. Barton, "Radar Clutter," Radars, vol. 5, Artech House, Dedham, 1977.

[4] E.C. Jordan and K.G. Balmain, Electromagnetic Waves and Radiating Systems, Prentice Hall, Englewood Cliffs, 1968.

[5] G.T. Ruck, D.E. Barrick, W.D. Stuart, C.K. Krichbaum, Radar Cross Section Handbook, Plenum, New York, 1970.

[6] A.J. Thomasian, The Structure of Probability Theory, McGraw-Hill, New York, 1969.


DATE
ILME